Number 503
9 June 2005

Contributions in Science

New Goatlike Camelid from the Late Pliocene of Tecopa Lake Basin, California

David P. Whistler and S. Davis Webb

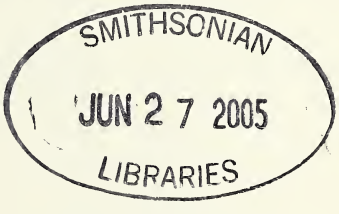

Natural History Museum
of Los Angeles County

Serial Publications of the Natural History Museum of Los Angeles County

The scientific publications of the Natural History Museum of Los Angeles County have been issued at irregular intervals in three major series; the issues in each series are numbered individually, and numbers run consecutively, regardless of the subject matter.

- Contributions in Science, a miscellaneous series of technical papers describing original research in the life and earth sciences.
- Science Bulletin, a miscellaneous series of monographs describing original research in the life and earth sciences. This series was discontinued in 1978 with the issue of Numbers 29 and 30; monographs are now published by the Museum in Contributions in Science.
- Science Series, long articles and collections of papers on natural history topics.

Copies of this publication are available through the Scholarly Publications Office at 213/763-3330 or by visiting our website at ⟨http://www.nhm.org⟩ for a PDF file version.

Natural History Museum of Los Angeles County
900 Exposition Boulevard
Los Angeles, California 90007

Printed at Allen Press, Inc., Lawrence, Kansas
ISSN 0459-8113

ERRATUM

In LACM Contribution number 503, we inadvertently misspelled the second author's name on the cover. We apologize for the error.

Number 503
9 June 2005

Contributions in Science

New Goatlike Camelid from the Late Pliocene of Tecopa Lake Basin, California

David P. Whistler and S. David Webb

Natural History Museum
of Los Angeles County

New Goatlike Camelid from the Late Pliocene of Tecopa Lake Basin, California

David P. Whistler[1] and S. David Webb[2]

ABSTRACT. We describe a unique new genus and species of camelid from the Late Pliocene sediments of the Tecopa Lake Basin south of Death Valley, California. A herd of at least fifteen individual camelids (young and old) were found embedded in standing position in gypsiferous mudstones of lacustrine origin. The quarry from which this sample was recovered occupied an area 5 by 12 m. The entombing sediments lay stratigraphically 3 m below a volcanic tuff that has been chemically correlated with the Huckleberry Ridge Ash radiometrically dated at about 2.1 million years ago. Most individuals were represented by fully articulated feet, fewer by epipodial elements, and very few by axial skeletal remains or cranial elements and dentition. The new genus and species *Capricamelus gettyi* displays an unusual combination of primitive and derived features. Among the former are its retention of large upper incisors and its permanently unfused metapodials (absence of cannon bones). Among the latter, its molars are hypsodont, transversely compressed, and increase greatly in length from the first to the third. The combination of features places this new taxon in the subfamily Miolabinae. Its most distinctive set of characters, including short, mountain goat–like limb proportions and powerful limb articulations, represent special adaptations for low-gear locomotion, unknown in any other camelids. Evidently the antiquity of the lineage leading to *C. gettyi* branched off from other miolabines at least 17 million years ago.

INTRODUCTION

The family Camelidae originated in North America some 46 million years ago as part of the middle Eocene radiation of selenodont artiodactyls. While ruminants were the principle products of this radiation in Eurasia, Camelidae was the dominant descendant on this continent. The prominent role of Camelidae during most of the Cenozoic in North America is comparable in many respects with that of Equidae. Both horses and camels greatly diversified during the Miocene Epoch, each family reaching its acme in the middle Miocene as it adapted to increasingly seasonal climates and open habitats in temperate North America. Near the end of the Miocene, both families dispersed to other continents where they survived while all of their North American sister taxa became extinct. As currently recognized, there are 36 valid genera of Camelidae (Honey et al., 1998) compared with 29 such genera of Equidae (MacFadden, 1998).

In the most recent revision of the Camelidae, Honey et al. (1998) recognized five subfamilies, of which Camelinae, including modern llamas and camels, is the most advanced. The most primitive subfamily group, aside from several basal twigs recognized simply as "primitive camelids," is the Stenomylinae ("gazelle camels"). Three other extinct subfamilies, all of which appear in the early Miocene, are the Floridatragulinae, Protolabinae, and Miolabinae.

In this contribution we place on record a new genus and species of miolabine camelid. It represents a much later survival of that subfamily than had previously been known. As we shall demonstrate, this last miolabine had developed several extreme adaptations, well beyond those known in other members of the subfamily. Most notably the distal part of the limbs had become extremely short, and the overall body proportions closely converged with those of true goats (ruminant subfamily Caprinae) and other goatlike ruminants. In recognition of this remarkable specialization, we introduce the informal term "goat camels" for this new genus and other miolabines that approach its condition. We believe that our description of this new genus of miolabine camelid will shed new light on the relationships of other members of its subfamily. Furthermore, it will help illuminate the relationships of the subfamily Miolabinae to other subfamilies within the multiple radiations of Miocene Camelidae (Honey et al., 1998). On the other hand, we note that a proper revision of the Miolabinae and its sister subfamlies lies well beyond the scope of this contribution.

In view of this overall history, it is quite astonishing to discover a hitherto unknown genus and species of camelid from the late Pliocene of the Tecopa Lake Basin near Death Valley, California. As demonstrated below, this new genus represents the last known representative of the subfamily Miolabinae. We conclude that this lineage branched off

1. Department of Vertebrate Paleontology, Natural History Museum of Los Angeles County, Los Angeles, California 90007

2. Division of Vertebrate Paleontology, Florida Museum of Natural History, University of Florida, Gainesville, Florida 32611

Contributions in Science, Number 503, pp. 1–40
Natural History Museum of Los Angeles County, 2005

quite early in the Miocene from known relatives and remained "hidden" in mountainous terrain of Western North America for some 20 million years.

METHODS

All specimens of the new camelid were recovered from the same locality with the use of jackhammers to remove the compact clayey matrix. All specimens described herein are catalogued in the Vertebrate Paleontology Collection of the Natural History Museum of Los Angeles County. As described in the section on taphonomy, the upright skeletons of a single herd were preserved differentially from the feet upward. Terminology for camelid osteology follows standard vertebrate paleontological usage (e.g., Webb, 1965). Features of camelid myology and arthrology referenced below are illustrated in Smuts and Bezuidenhout (1987).

Because of the mode of burial and preservation, cranial and dental material is limited. Tables 1 to 11 provide morphologically important measurements from the few available specimens. Most measurements cannot be duplicated in multiple specimens. More detailed measurements that provide additional information about proportions within crania are provided in the text. The excellent preservation and adequate sample size of the manus and pes provided an especially valuable set of meristic data. All measurements were taken with a Vernier caliper to the nearest 0.1 mm. The phalanges occurred uniformly as articulated sets, often associated with the manus or pes. After several trial samples, we determined that both in the manus and pes, the proximal, median, and ungual phalanges of digit III were symmetrical in all dimensions with those of digit IV. Having confirmed that the two sides of these paraxonic feet were mirror images of one another, we arbitrarily selected digit III for measurements of both manual and pedal phalanges. Standard statistical analyses of skeletal measurements were carried out with the Excel software program.

ABBREVIATIONS AND TERMINOLOGY

AMNH	American Museum of Natural History, New York, New York
F:AM	Frick collection of the American Museum of Natural History, New York, New York
LACM	Natural History Museum of Los Angeles County, Los Angeles, California
ka	Thousands of years before present
L	Left
Ma	Meganna, or millions of years before present
R	Right

Individual teeth from the upper dentition are referred to with a superscript number, for example M^2 is the second upper molar; lower teeth are cited with subscript numbers.

GEOGRAPHIC SETTING

Tecopa Valley is an intermontane basin situated in the southwestern portion of the Basin and Range Province of interior western North America (Fig. 1). The valley is approximately 24 km long and 17 km wide at its southern end. Average elevation of the valley floor is between 400 and 500 m.

The valley is immediately surrounded by mountains with average elevations of 1500 m, but nearby mountain ranges reach elevations of 3650 m. The present-day course of the ephemeral Amargosa River, with a source in the mountains of south-central Nevada and a terminus in the Death Valley Basin, traverses the Tecopa Valley. The late Pliocene and Pleistocene deposits within the Tecopa Lake Basin were downcut and dissected by the Amargosa River during the late Pleistocene, producing approximately 300 km^2 of dissected badlands on the valley floor.

GEOLOGIC SETTING

Prior to the late Pleistocene breach of the Tecopa Lake Basin at about 186,000 years ago, the Tecopa Valley served as the terminus of the Amargosa River for more than 5 million years, producing Lake Tecopa (Dohrenwend, 1985; Dohrenwend et al., 1991; Morrison, 1999). Detailed studies over the past decade have revealed a complex history of playa, freshwater lake, and hypersaline lake for Lake Tecopa (Morrison, 1991; Larson et al., 1991; Morrison, 1999; Larson, 2000).

The general stratigraphy of the deposits has been established by Sheppard and Gude (1968) and Hillhouse (1987). More recent refinements are provided by Morrison (1991, 1999) and Larson (2000). Deposits comprise a series of lacustrine and marginal fluviatile deposits that accumulated in what is today called the Tecopa Lake Basin (Chesterman, 1973; Hillhouse, 1987). The lacustrine deposits are composed of a variety of gypsiferous mudstones, siltstones, and tufa (subaerial and freshwater limestone), with basin marginal deposits of sandstone and conglomerate. The lacustrine sequence also contains a number of distinctive volcanic tuff layers that have been extensively studied and correlated to source areas of well-constrained ages (Shepard and Gude, 1968; Sarna-Wojcicki et al., 1987). These tuffs form distinctive marker beds that can be used to correlate sections throughout the Tecopa Lake Basin. In addition to the distinctive tuff beds, most of the fine-grained sedimentary facies are tuffaceous. Maximum exposed thickness within the lacustrine facies is about 100 m.

Hillhouse (1987) was the first to describe and map the Quaternary geology within the Tecopa Lake Basin in detail. Morrison (1991, 1999) has provided more detail and named a sequence of alloformations (North American Stratigraphic Code, Article 58) within the Lake Tecopa Allogroup. Many of the alloformation boundaries are defined on the basis of the distinctive tuff marker beds.

FOSSIL OCCURRENCES AND AGE

Fossil vertebrates are known from several stratigraphic levels within the sediments deposited in the Tecopa Lake Basin (James, 1985; Reynolds, 1991; Woodburne and Whistler, 1991). Most of the fossils from the lake beds have been recovered from a restricted area in the southeastern portion of the basin. The larger mammals are dominated by a di-

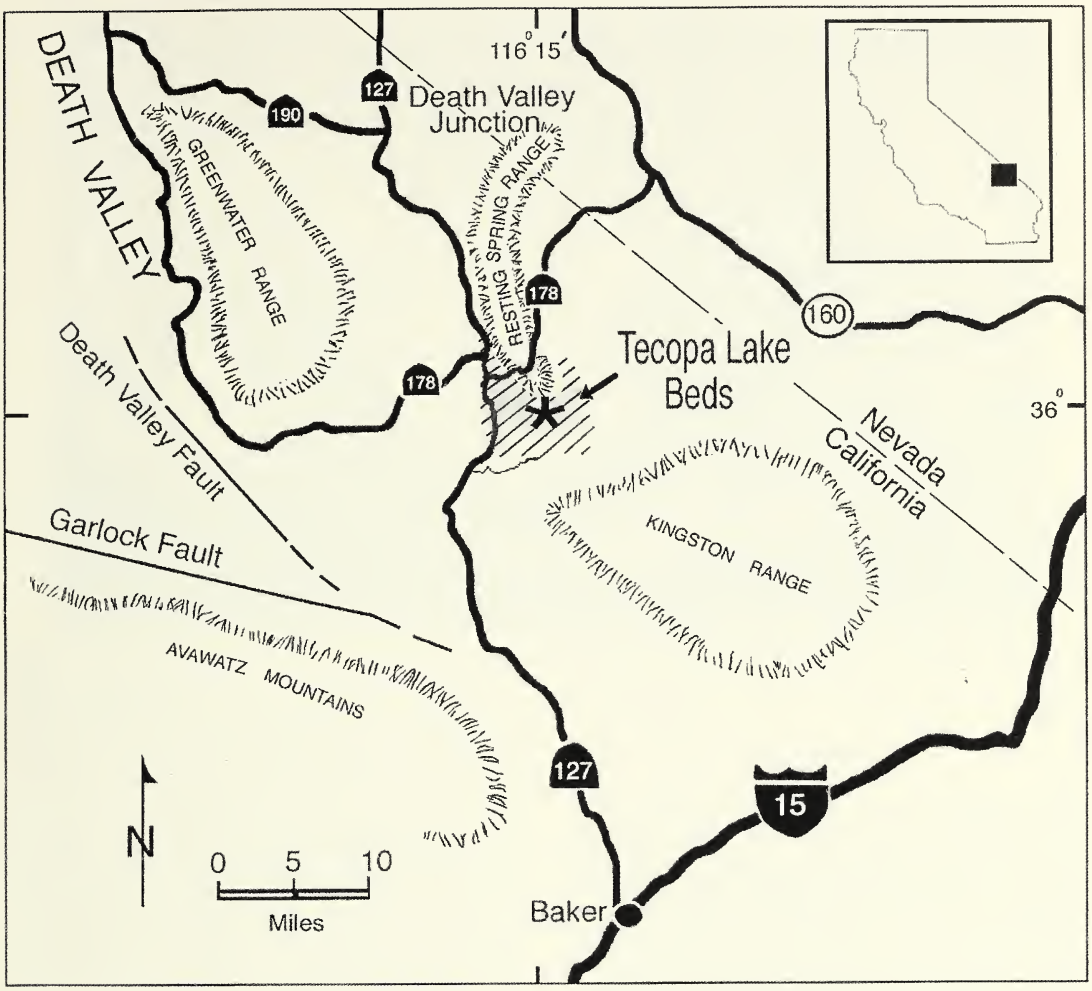

Figure 1 Index map illustrating location of Tecopa Lake Basin and Tecopa Lake Beds. Star is general location of fossil occurrences

versity of camels (*Camelops* sp. Leidy, 1854), short- and long-legged species referred to *Hemiachenia* Gervais and Ameghino, 1880, and *Capricamelus gettyi,* the new genus and species described herein. There are also two kinds of equids (one burro-sized, one quarter horse–sized), an antilocaprid, a mastodon, and *Mammuthus* sp. The only carnivore in the fossil assemblage is a moderate-sized fox. The small vertebrates are represented by two shrews (*Sorex* sp. and *Notiosorex* sp.), a rabbit (*Hypolagus* cf. *H. limnetus* Gazin, 1934), a ground squirrel (*Spermophilus* cf. *S. bensoni* (Gidley, 1922)), two species of kangaroo rat (*Dipodomys* sp.), a white-footed mouse (*Peromyscus* sp.), a cotton rat (*Sigmodon* sp.), and a pack rat (*Neotoma* sp.). Birds are represented by a flamingo (cf. *Phoenicopterus* sp.).

The fossils recovered from the lake beds, including *C. gettyi,* were recovered a few meters below the Huckleberry Ridge Tuff (2.1 Ma) (Sarna-Wojcicki et al., 1987) from near the base of the exposed section in the upper part of the Spanish Trails Alloformation of Morrison (1999). Other prominent tuffs within the Lake Tecopa Allogroup include the Lava Creek B Tuff (665 ka) and the Bishop Tuff (758 ka) (Sarna-Wojcicki et al., 1987; Morrison, 1999). The top of the Spanish Trails Alloformation is defined by the Huckleberry Ridge Tuff; thus, the assemblage is slightly older than 2.1 Ma, or late Blancan North American land mammal age.

Paleomagnetic studies in the Tecopa Lake Basin by Hillhouse (1987) and Valet et al. (1988) have recognized the Reunion geomagnetic subchron (2.15–2.14 Ma; Van Couvering, 1997) at the top of the Spanish Trails Alloformation, providing independent confirmation of the tephrochronologic age determinations. Larson and Patterson (1993) sampled for the 2.6 Ma Gauss-Matuyama chron

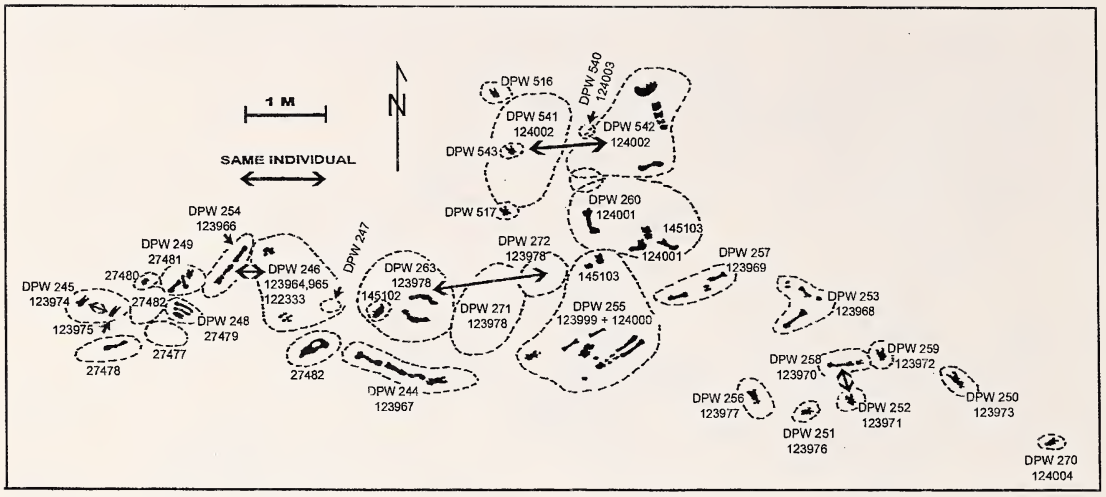

Figure 2 Quarry map for locality LACM 7111. Numbers preceded by initials "DPW" are field numbers of individual field jackets. Five- and six-digit numbers are LACM specimen numbers. Double-pointed arrows connect jackets that contained associated skeletal elements of single individuals

boundary but did not find it in the exposed sediments.

TAPHONOMY

One concentration of smaller vertebrate fossils was recovered from a restricted lens with the bones scattered throughout the bed. Most of the other fossils were recovered as isolated specimens scattered over an approximately 4-km^2 area. Preservation of the isolated larger bones was unusual in that the most common material recovered is fully articulated feet and lower legs found embedded in a standing position. Other body skeletal parts are rare. The fossil quarry (locality LACM 7111) that yielded the new camel, described herein, in particular demonstrates this selective form of preservation (Fig. 2). Fully articulated feet, and in some cases, parts of legs of at least 15 individual camels (young and old) were found embedded in standing position in the lake muds in a restricted area of 5 by 12 m. Highly fractured and weathered partial skeletons were found connected to only two sets of the feet. One such example is shown in Figure 3. Within 100 m of this fossil quarry were found five other occurrences of camel legs and feet preserved in standing position. Because of this mode of preservation, this fossil producing area was dubbed "Standing Camel Basin."

This unusual mode of preservation has been interpreted as being the result of animals becoming mired in the muds along the shore of ancient Lake Tecopa. Once trapped, the animals probably struggled until they died of starvation. The legs mired in the mud were subsequently preserved, while the bodies and skulls became subject to disintegration by weathering. One phenomenon present with the Tecopa Lake Basin today may further explain these unusual fossil occurrences. Thermal springs are present along a lineation that crosses the basin. These springs produce localized wet areas that tend to collect fine sand and silt moved around by aeolian processes. This fine material supports a localized area of vegetation (mostly grasses), and the two combine to form a somewhat firmer "caprock" over the source of upwelling spring water. Below this caprock is an area of water-saturated lake mud. This caprock can support the weight of smaller animals, but heavier ones (such as a human) break through the cap and find themselves immediately embedded deeply in saturated "quick mud." If these springs existed 2 million years ago, the vegetation would have attracted animals who would unwittingly have become trapped.

Standing Camel Basin is aptly named, both for the animals' stances and for the most abundant species of the entrapped taxa. Evidently, the camels were mired down instantly as they plunged feet first into unctuous clay. The perfect articulation of every bone and sesamoid is further evidence of this near instantaneous burial. This suggests that the deep clay mire was disguised by a thin surface of drier material that deceived the camels. Two skeletons also were on the bank together at one end of the mud deposit.

The depth to which the camels plunged into the mud is not entirely clear. A set of minimum depths can be deduced from the degree of preservation of vertically aligned articulated limbs. About a third of the articulated specimens consist only of the foot, from the carpus or tarsus through the metapodials to the ungual phalanges. Another third of the limbs include at least part of the propodial elements along with all more distal elements. The upper end of such specimens gives evidence of erosion

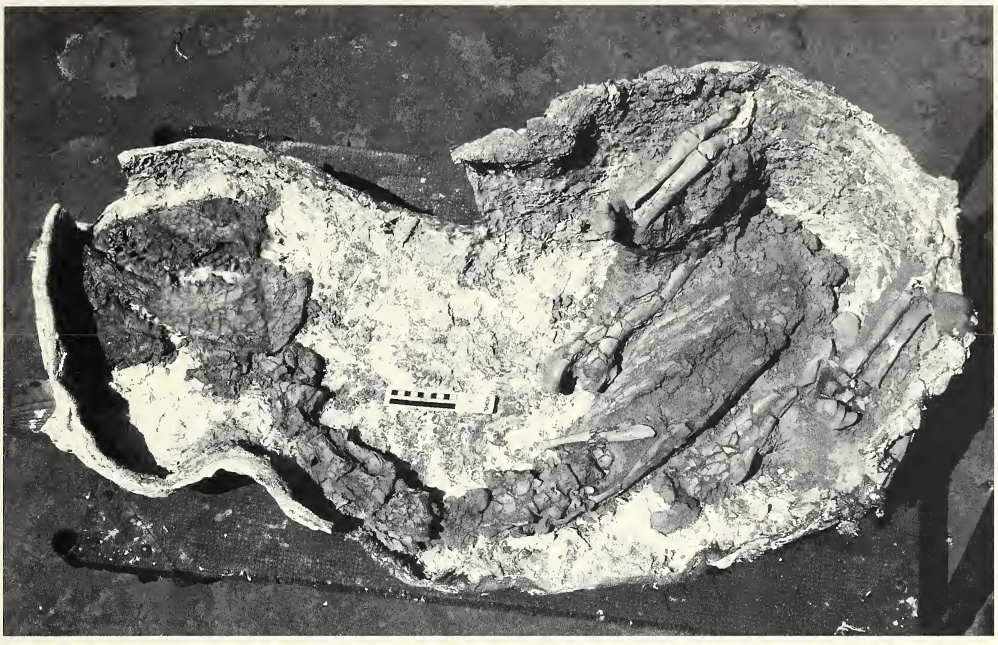

Figure 3 *Capricamelus gettyi,* field jacket DPW 542 containing anterior portion of holotype skeleton, LACM 124002. Jacket prepared from ventral side. Note articulation of L and R manus and fracturing of more proximal limb elements and axial skeleton

and diagenetic breakage from postmortem desiccation and shrinkage of the volcanic-rich clay deposits, whereas the distal elements are virtually perfect and include all four sesamoid bones in their correct positions (Figs. 12C, 16C).

SYSTEMATIC PALEONTOLOGY

Mammalia Linnaeus, 1758

Artiodactyla Owen, 1848

Neoselenodontia Webb and Taylor, 1980

Tylopoda Illiger, 1811

Family Camelidae Gray, 1821

Subfamily Miolabinae Hay, 1902

***Capricamelus,* gen. nov.**

***Capricamelus gettyi,* sp. nov.**
Figures 3–17, 19; Tables 1–11

HOLOTYPE. Nearly complete skeleton of an adult individual, LACM 124002.

HYPODIGM. The paratype is a nearly complete skeleton of an adolescent individual, LACM 123978. The rest of the collection, dominated by distal sets of articulated limb elements of at least 15 individuals, is listed in Appendix 1.

ETYMOLOGY. *Capri* = goatlike; *camelus* = camel. The genus name indicates that this camelid has mountain goat limb proportions; *gettyi* = named in recognition of Mr. Andrew R. Getty, whose support and interest greatly facilitated this study.

TYPE LOCALITY. Standing Camel Quarry, LACM locality 7111, from late Blancan sediments in Tecopa Lake Basin south of Death Valley, California.

AGE AND DISTRIBUTION. Late Blancan (late Pliocene) from the Spanish Trails Alloformation, about 2.1 Ma as discussed in "Geologic Setting." Also two isolated occurrences in Nevada, each based on a single podial element, one from the late Rancholabrean (late Pleistocene) of Smith Creek Cave and the other from sediments of unknown age on Mormon Mesa, Nevada. These occurrences are further detailed at the end of the "Description" section.

DIAGNOSIS. *Capricamelus gettyi* falls within the subfamily Miolabinae and differs from all other Camelidae in presenting a broad rostrum with an enlarged pair of upper incisors and a mandible with a vastly expanded posteroventral apron with no angular hook and a low coronoid process. *Capricamelus gettyi* differs from all other Miolabinae in the reduction of its teeth to the dental formula I 2/3 C 0/0-1 P 1/1 M 3/3, and in the failure of its third and fourth metacarpals, as well as its third and fourth metatarsals to fuse into cannon bones. *Capricamelus gettyi* is further distinguished by the following characters: *Lama*-sized camelid with enlarged facial region and very long premaxillary that wedges far between nasal and maxillary bones;

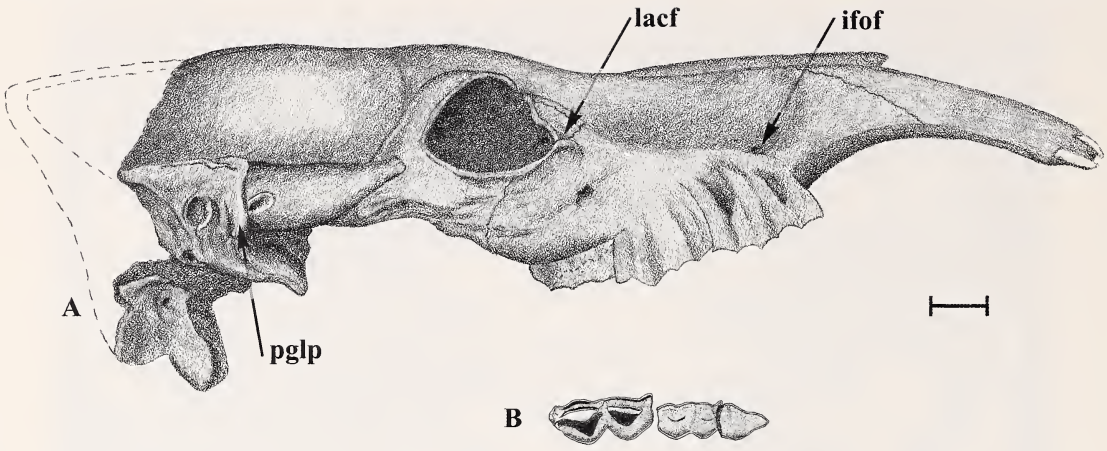

Figure 4 *Capricamelus gettyi,* paratype, juvenile cranium, LACM 123978. **A,** lateral view; **B,** occlusal view of dentition with DP^{3-4}, M^1. **Abbreviations:** ifof = infraorbital foramen, lacf = lacrimal fossa, pglp = postglenoid process. Scale bar = 1 cm

large lacrimal fossa; large subcircular postglenoid process not encroaching on auditory bulla; bulla deep and laterally compressed; mandible with very long diastema; long shallow symphysis; single (anterior) mental foramen; molars elongate, transversely compressed, very hypsodont, with light cementum, flattened labial walls in uppers and flattened lingual walls in lowers; cervical vertebrae about 20% shorter than in comparably sized *Lama guanicoe* (Muller, 1776); limbs distally abbreviated, resembling the proportions of "true rock climbers" such as mountain goats; metapodials half as long, relative to epipodials, as in other camelids; distinct second metacarpal and metatarsal bones; ungual phalanges with strong opposing medial flanges.

DESCRIPTION. Cranium (Figs. 4A, 5A–B, 6A; Table 1). The adolescent paratype skeleton, LACM 123978, provides most of the available evidence of cranial morphology. Despite being crushed laterally during diagenesis, the right side of its cranium is nearly complete. The cranium of the holotype, badly crushed and eroded, confirms the cranial proportions in a fully mature individual. Two other skull fragments supplement the two types, as noted where appropriate.

The cranial length of the adolescent skull, LACM 123978, is about equally divided between the facial/rostral portion, anterior to the orbits, and the braincase, including the orbits. These proportions contrast markedly with those of extant camelids in which the facial portion accounts for only about 40% of skull length. The premaxillary accounts for a substantial part of the unusually elongated face of *C. gettyi.* It forms a large trapezoid about 140

Table 1 Measurement of selected cranial features.

	Measure (mm)			
	LACM 124002	LACM 123978	LACM 27480	LACM 27482
Length, I^1 to occipital condyle		390		
Premaxillary length	28			
Premaxillary height above alveolar border		26		
Premaxillary width, rostral end			48.4	
Length, premaxillary symphysis			52.2	
Length nasal		105		
Anterior width nasal		>8		
Distal width nasal		23.4		
Width postorbital bar		>20		21.4
Diameter, maxillary fossa		30		
Depth jugal		9.5		39.5
Dorsoventral height, external auditory meatus		8.7		
Anteroposterior length, external auditory meatus		6.5		

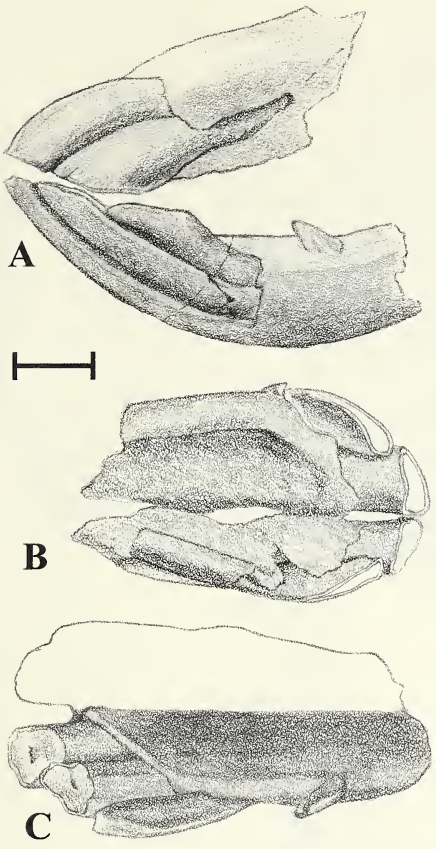

Figure 5 *Capricamelus gettyi,* adult referred specimen, LACM 27480. **A,** left lateral view, associated rostrum, and anterior mandibular symphysis with two upper and three lower incisors and lower left canine; **B,** ventral view, rostrum; **C,** dorsal view, left mandibular symphysis. Scale bar = 1 cm

mm long, rising about 26 mm above the alveolar border in the paratype and 28 mm in a mature specimen, LACM 27480 (Figs. 5A–B). The premaxillary wedges far posteriorly between the nasal bone above and the maxillary below, separating them for a distance of 48.7 mm. The posterior tip lies about 60 mm above the anterior portion of DP^4. The premaxillary bone also extends posteriorly along the alveolar border for a distance of about 48 mm, which is about half the length of the long diastema.

The great enlargement of the premaxillaries in *C. gettyi* presumably reflects their support of the powerful pair of procumbent upper incisors described below. The rostral ends of the premaxillaries are very deep and transversely broadened across the roots of the incisors, in striking contrast to the delicately tapered rostrum of virtually all other described camelids. In LACM 27480 the premaxillaries span a width of 48.4 mm at their rostral end. Posterior to the incisor roots the rostrum narrows slightly. On the palatal surface of the adolescent paratype skull, the large pair of palatine fissures open 47.1 mm posterior to the anterior margin of the premaxillaries.

The nasal bone is about 105 mm long, less than 8 mm wide anteriorly, and gently arched dorsally. It broadens posteriorly to a width of 23.4 mm along the frontal suture. The posterolateral corner of the nasal meets the posterodorsal edge of the maxillary at a small lacrimal vacuity.

The frontal bone forms a short but very broad dorsal expanse above the maxillary and lacrimal bones, where its maximum width is about 130 mm in the immature paratype and evidently more in the mature type. The frontal extends laterally to form the dorsal and posterior portions of the widely projecting orbit. The postorbital bar is not only complete, but also quite wide (Figs. 4A, 6A). The parietal is not well enough preserved to describe.

The lacrimal bone is 12.4 mm high and 13.7 mm wide in its facial expanse. An even greater rectangular portion of the bone, measuring about 12 mm high and 17 mm wide, forms the anterodorsal wall inside of the orbit. The lacrimal fossa is 6.5 mm tall and leads into the lacrimal foramen.

The maxillary covers a very large trapezoidal expanse ventral to the nasal, posteroventral to the premaxillary, and anterior to the orbit. The maxillary also meets the lacrimal posterodorsally and the jugal posteroventrally. On the alveolar border, the maxillary also meets the premaxillary at about the middle of the long diastema between the incisors and the DP^4, as noted above. The infraorbital foramen opens about 30 mm dorsal to the anterior end of DP^4. That foramen defines the anteroventral border of a large, shallow maxillary fossa. Posteriorly the maxillary forms the anteroventral third of the orbit, and posteroventrally it meets the jugal along a nearly vertical suture about 10 mm deep. It supports a strong crest for the origin of *M. masseter,* but unfortunately the exact length cannot be determined because of crushing of the bone in that region. The alveolar portion of the maxillary bone extends far posteriorly inside the ventromedial portion of the orbit where it encloses the developing last molar.

The jugal forms the deep arcuate, ventral margin of the orbit, rising anteriorly to a maximum height where it meets the maxilla. In a mature fragment of the orbital region, LACM 27482 (Fig. 6A), the jugal attains a maximum depth at the squamosal contact. Posteriorly it divides so that its dorsal branch separates the squamosal from the frontal. The ventral process becomes thinner as it continues posteriorly, terminating just anterior to the glenoid fossa. The jugal thus spans a total distance of 16.0 mm along the ventral border of the zygomatic arch.

The zygomatic process of the squamosal reaches a depth of 23.3 mm in LACM 27482 as it deepens rapidly from its shallow anterior contact with the jugal. The zygomatic process is 70.0 mm long as measured along its dorsal margin.

In the auditory region the squamosal presents a

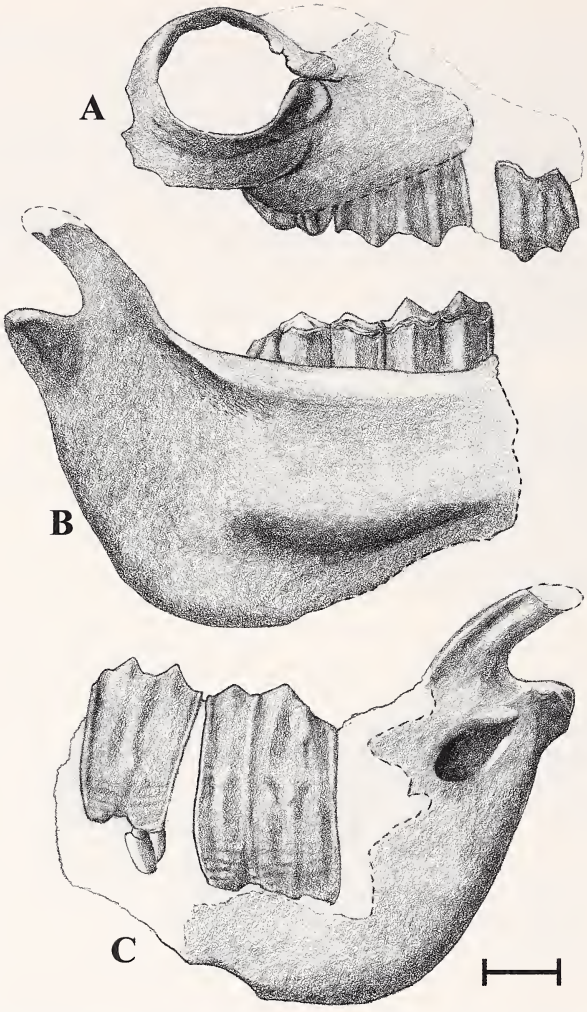

Figure 6 *Capricamelus gettyi,* adult referred specimen, R mandible, LACM 27482. **A,** associated cranial fragment view; **B,** labial view; **C,** lingual view. Scale bar = 1 cm

large, triangular, and remarkably plain, lateral exposure. In the paratype skull the dorsal margin of the squamosal extends about 44 mm from the base of the postglenoid process to the mastoid suture with the exoccipital. The external auditory meatus has only a minor bony lip anteroventrally. In the holotype skull (LACM 124002) the meatus is slightly smaller, but has a much thicker rugosity along its anterior and ventral margins. In the paratype skull the massive postglenoid process is about 24 mm wide and projects 13.1 mm ventral to the glenoid fossa. In the holotype skull the postglenoid process has similar morphology, but is even larger. The postglenoid forms a large subcircular process that lies completely free of the adjacent bulla and allows broad passage of the postglenoid canal.

The most remarkable feature of the squamosal region is the deep, laterally compressed auditory bulla. Each of the two type specimens provides partial evidence of the bulla and the adjacent petrosal bone. In the paratype the lateral portion of the bulla is well preserved and extends 37.4 mm ventral to the external auditory meatus. The lateral portion of the bulla is only 8.0 mm thick transversely. The tympanohyal recess lies 17.0 mm above the ventral tip of the bulla, tightly pocketed within the lateral wall. The holotype preserves the upper edge of the left petrosal and a distal portion of the medial wall of the left bulla lying about 55 mm ventral to the external auditory meatus. This partial bulla also preserves the tympanohyal recess, which marks the anterior division between the two parts of the bulla. Taken together, these two fragmentary bullae confirm the reconstruction of *C. gettyi* bulla as deep, pendulous, and transversely compressed. The right side of the paratype skull (Fig. 4A) clearly shows that the bulla extended well below the alveolar plane of the molars. It is less certain whether it

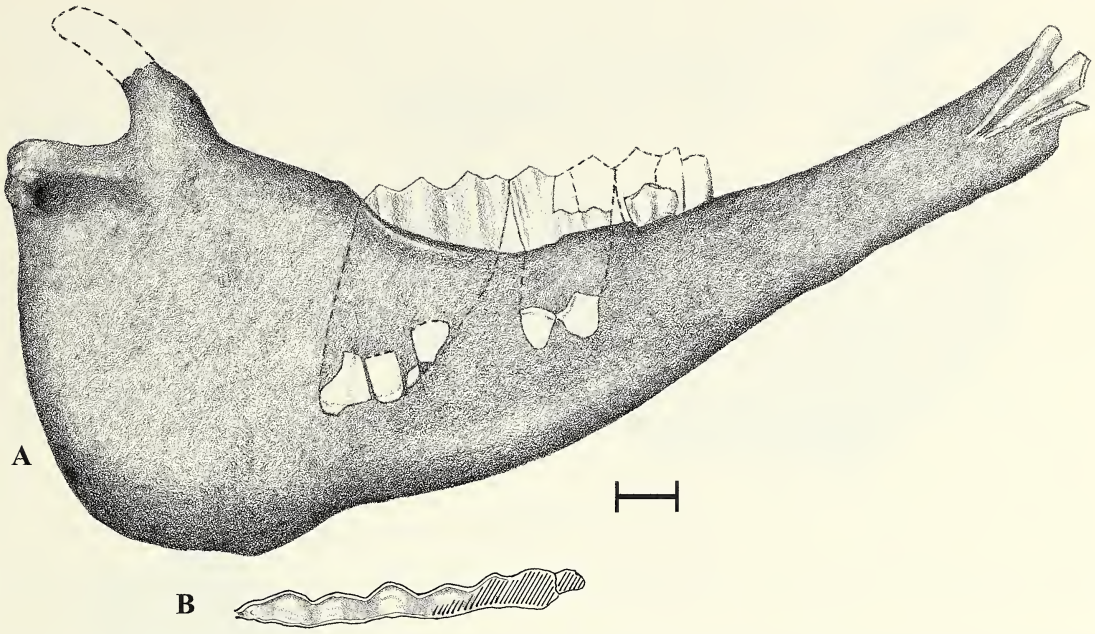

Figure 7 *Capricamelus gettyi,* holotype, L mandible, LACM 124002. A, lingual view; B, occlusal view of dentition including partial M_{1-2}, complete M_3. Diagonal lines in panel 7B indicate broken tooth crowns. Scale bar = 1 cm

reached ventrally beyond the paroccipital process, since that element is not preserved, but that conclusion seems probable in view of the great vertical extent of the bulla.

The incus and the head of the malleus were recovered from the epitympanic recess of the middle ear cavity in the paratype skull. The maximum dimension, taken across the short and long processes of the incus is 3.6 mm.

The paratype cranium also preserves a major portion of the occiput, from the left occipital condyle dorsally to the upper third of the exoccipital. The condyle is nearly 30 mm in dorsoventral diameter and nearly 16 mm at its greatest width. A small mastoid foramen occupies a shallow concavity at the dorsomedial margin of the condyle. The mastoid process was evidently weakly developed. The area of the paroccipital process is missing, and the lateral margin of the exoccipital is preserved to a point only 31.0 mm above the external auditory meatus.

Mandible (Figs. 5A,C, 6B–C, 7A, 8A,C; Table 2).The diastema in the mature holotype is remarkably long due to the absence of a lower canine. The mental foramen in the paratype lies about 8 mm dorsal to the ventral border of the horizontal ramus at a point just anterior to the thickened posterior edge of the symphysis. The paratype mandible shows clearly the absence of a posterior mental foramen in the area below the anterior cheek teeth. The angular region is immensely expanded, so that the oblique distance from posterior end of the oc-

Table 2 Measurement of selected mandibular features.

	Measure (mm)			
	LACM 124002	LACM 123978	LACM 27480	LACM 27482
Length (not including procumbent incisors)	353	262.5		
Depth below anterior lobe, M_3	79.5			
Diastema length	100.8	58.6		
Diastema depth at midpoint	38.1	23.4		
Symphysis length		53.7	65	
Symphysis depth		13	21	
Coronoid process length		25.9		27.2
Height, mandibular condyle above ventral border of mandible		106	102	

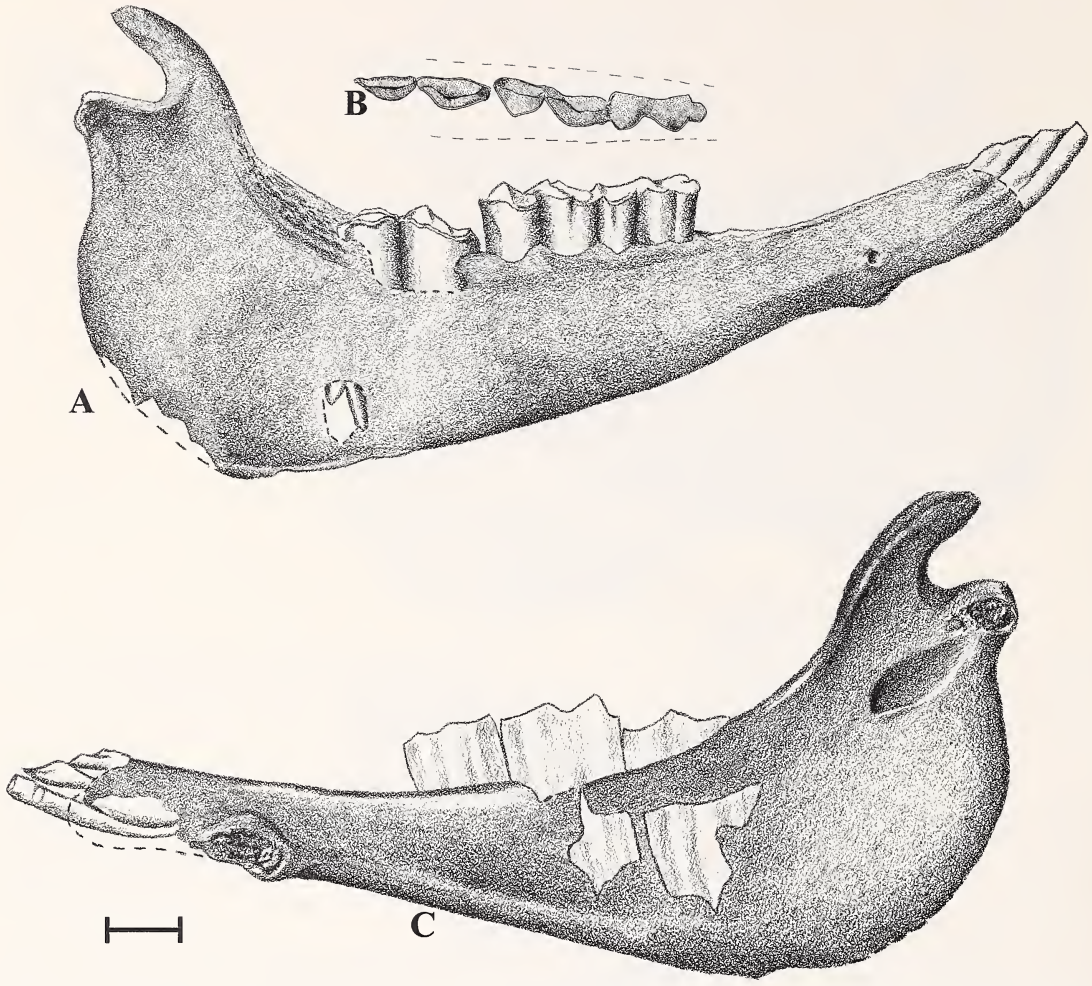

Figure 8 *Capricamelus gettyi*, juvenile paratype, R mandible, LACM 123978. A, labial view; B, occlusal view teeth; C, lingual view of mandible including DP_4, M_{1-2}. Scale bar = 1 cm

clusal surface of M_3 to the posteroventral margin of the angle is 131.3 mm. In the immature paratype with M_3 unerupted that distance is only about 80 mm.

The ascending ramus of the mandible presents two unusual features which are shared among camelids only with some Stenomylinae and Miolabinae. First is the absence of an angular process or hook. Its absence from the expansive curve of the angular region is clearly confirmed in both the holotype and the paratype (Figs. 7A, 8A,C). Second, the coronoid process is remarkably short. The tip of the coronoid in the paratype lies just 18.1 mm dorsal to the mandibular condyle. In extant *Camelus dromedarius* Linnaeus, 1758, by contrast, the coronoid process is about 50 mm tall.

As in other camelids there are two articular surfaces of the mandibular condyle. In the holotype mandible, the dorsal articular surface consists of a broad elliptical area that is slightly convex dorsally and measures 37.2 mm transversely by 18.3 mm anteroposteriorly. The caudal articular surface is triangular, slightly concave, and measures about 22 mm transversely by about 16 mm dorsoventrally. The medial side of the ascending ramus provides a large concave surface for the insertion of the *M. pterygoideus* almost equal to the expanse on the lateral side for the *M. massetericus*. The dental canal, 7.5 mm in diameter, emerges from the medial wall of the jaw 20.0 mm anteroventral to the mandibular condyle.

Based on the characters observed on the four cranial specimens discussed above, we have attempted a reconstruction of the adult skull of *C. gettyi* presented in Figure 9.

Dentition (Figs. 4B, 5A–C, 7B, 8B; Tables 3–4). The dental formula in *C. gettyi* is; I 2/3 C 0/0-1 P 1/1 M 3/3. With the addition of smaller upper and lower third premolars, the deciduous dental formula is DI 2/3, DP 2/2.

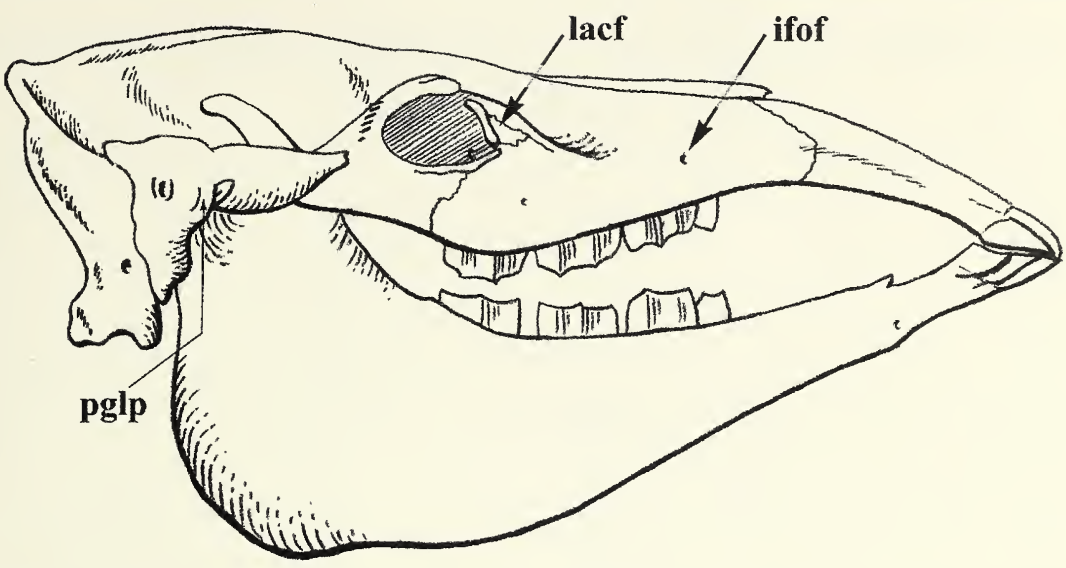

Figure 9 Restoration of adult skull of *Capricamelus gettyi*. **Abbreviations:** ifof = infraorbital foramen, lacf = lacrimal fossa, pglp = postglenoid process

The two pairs of upper incisors form an immense, procumbent arcade that wears heavily against the three pairs of lower incisors (Fig. 5A). The second incisor in LACM 27480 has a long, gently curved wear face that becomes progressively narrower posteriorly. This expansive second upper incisor occludes with both the second and third lower incisors. The enamel of the upper incisors is thick on their convex anterior faces and much thinner on their slightly concave posterior faces. The enamel crowns of the incisors are very long.

The lower incisor arcade consists of three pairs

Table 3 Measurement of upper dentition.

	Measure (mm)			
	LACM 123978	LACM 27480	LACM 27482	LACM 145102
Width, upper incisor battery		50.8		26
I^1 crown, md		8.0		
I^1 crown, lb/lg		5.6		
I^1 ch		41.0		
I^2 md		24.5		
I^2 lb/lg		5.6		
I^2 ch	~25	>51		
DP^3 ap	19.4			
DP^3 lb/lg	13.9			
DP^3 ch	9.6			
DP^4 ap	15.2			
DP^4 lb/lg	15.5			
DP^4 ch (midlabial)	15.2			
M^1 ap	35.6		30.5	
M^1 lb/lg	18.6			
M^1 ch (lingual)	48.9		41.4	
M^2 ap			40.7	
M^2 ch (lingual)			43.3	
M^3 ap			36.4	
M^3 ch (lingual)			43.9	

Abbreviations: ap, anteroposterior; ch, crown height; lb/lg, labiolingual; md, mesodistal

Table 4 Measurements of lower dentition.

	Measure (mm)			
	LACM 124002	LACM 123978	LACM 27480	LACM 27482
I_1 md			11.8	
I_1 lb/lg			14.1	
I_2 md			10.4	
I_2 lb/lg			15.3	
I_2 ch			>51	
I_3 md			7.1	
I_3 lb/lg			17.6	
C ap			7.4	
C lb/lg			5.9	
DP_4 ap		25.7		
DP_4 lb/lg		11.4		
DP_4 ch		16.2		
P_4 ap	12.4			
P_4 lb/lg	9.5			
M_1 ap	~20	29.5		
M_1 lb/lg		11.6		
M_1 ch (lingual)		46		
M_2 ap	43.3	37.5		39.5
M_2 lb/lg	14.5	11.8		16.7
M_2 (lingual)	~56	56.0		53.3 (labial)
M_3 ap	47.5			47.0
M_3 lb/lg	42.2			15.6
M_3 ch (lingual)	~63.6			63.6 (labial)

Abbreviations: ap, anteroposterior; ch, crown height; lb/lg, labiolingual; md, mesodistal

of large procumbent incisors. They occlude fully with the upper arcade. The composite wear surface is slightly convex dorsally and slightly concave ventrally. As in the uppers, the lower incisors have thick enamel on their anterior faces and much thinner enamel on their posterior faces.

Two sets of deciduous incisors are present in this sample, but most are badly shattered. These milk teeth develop essentially the same relationships as in the adult incisors, even though they are shorter crowned and far more delicately constructed. LACM 145102 presents two pairs of long, delicate upper deciduous incisors which form an arcade about 26 mm wide that occlude with their three pairs of lower counterparts. The paratype right mandible (LACM 123978) clearly indicates the features of the deciduous lower teeth, which resemble delicate miniatures of the permanent lower incisors (Figs. 8A,C). The tip of the unerupted crown of permanent I_1 lies between the roots of DI_1 and DI_2. The unworn enamel crown of I_2 is about 25 mm long, and that of DI^3 is about 20 mm long, indicating that even the deciduous teeth were fully developed as specialized nipping teeth.

The only evidence of any canine tooth is the partly erupted left lower canine in LACM 27480, a mature individual with permanent incisors fully erupted (Figs. 5A,C). In addition this specimen has an alveolus representing an equivalent tooth on the right side of the same mandible. The mature mandible of the holotype shows no evidence of a canine tooth (Fig. 7A).

The left P_4 of the holotype mandible is heavily worn and narrows to a point anteriorly (Fig. 7B).

Two upper and two lower deciduous premolars are preserved in the paratype cranium, LACM 123978. The left DP^3 of the paratype specimen is two-rooted and triangular (Fig. 4B). The labial wall of the crown is slightly convex. There is on this tooth, as on all the cheek teeth, a light cover of cementum. The left DP^4 is a two-lobed, quadrate tooth with four slender roots (Fig. 4B). It is essentially a smaller, lower crowned version of the upper molars described below. Both fossettes within the crown are nearly worn away. The labial wall of the tooth is nearly flat, with a very weak parastylar rib and no mesostyle.

The DP_3 in the left mandible of the paratype is represented by a two-rooted alveolus 9.0 mm long. A badly broken right DP_3 in LACM 145102 confirms the nature of this tooth. The paratype provides a well-preserved example of a three-lophed DP_4 (Fig. 8B). Its anterior lophid is turned lingually. The lingual wall of this molariform tooth is essentially flat with a thin surface of cementum. The same size and morphology are confirmed by a broken DP_4 in LACM 145102.

Evidence of the permanent premolars in this new

Table 5 Measurements of vertebral lengths.

	Measure (mm)			
	LACM 124002	LACM 124001	LACM 123978	LACM 145103
Atlas	52.9			
Axis	94.5			
C3	84.1			
C4	76.3			
C5	72.3			
C6	68.6			
C7	72.8			
T1 (less epiphyseal plate)			19.5	
T2 (less epiphyseal plate)			20	
L4				43.8
L5				46.2
L6				46.8
L7		46.1		47.6
S1		40.3		
S2		35.6		
S3		35.1		
C1		29.8		
?C2		19.4		

genus and species is sparse. In the left mandibular ramus of the holotype cranium, P_4 is represented by two alveoli, of which the anterior is smaller than the posterior. These probably indicate a short triangular premolar (Fig. 7B). There is no evidence of any other alveoli anterior to P_4. On this basis we infer the greatly reduced premolar dental formula.

The holotype cranium is badly crushed in the area where an equivalent upper premolar should occur. Although this sample does not provide any upper premolar, we can predict the presence of P^4 because it produced wear on its lower occluding partners, the anterior lobe of M_1 and all of P_4. Also, we infer the absence of an upper third premolar from the reduced nature of P_4. Thus we suggest that the upper premolar formula mirrored that of the lower.

The molars of *C. gettyi* are transversely compressed and very hypsodont. The molar lengths increase substantially from front to back, although not as dramatically as in such progressive stenomyline camels as *Rakomylus* Frick, 1937, or *Blickomylus* Frick and Taylor, 1968. The upper molars arch lingually along the lengths of their crowns, in a manner reminiscent of pliohippine horse molars. Likewise the lowers bow out labially, although somewhat more subtly, along their crown heights. All of the cheek teeth, as noted above, bear a thin layer of cementum.

The upper molars tend to increase in size and hypsodonty along the tooth row (Table 3). LACM 27482 most readily indicates this trend (Fig. 6A). Their transverse dimensions are more difficult to ascertain but range between about 17 and 21 mm as measured near the apices of the molar crowns. Their maximum crown heights are measured along the lingual slopes simply because their labial faces were not exposed. Each of the upper molars has a very faint set of five ridges, representing the parastyle, mesostyle, metastyle, and two intervening ribs, extending down its labial wall. These same dimensions are confirmed in approximate manner by holotype and paratype specimens. The nearly unworn right M^1 of the paratype is slightly larger than in LACM 27482 (Table 3).

The lower molars attain similar heights but are consistently narrower (Table 4). The M_2 is unerupted in the paratype mandible (Figs. 8A,C). The posterior part of a right mandible, LACM 27482, provides the best preserved examples of the last two molars (Figs. 6B–C; Table 4). Their lingual walls are nearly flat. The anterolabial and anterolingual stylids are prominent on the last molar. The inflections between the molar lophids are deep and angular.

Vertebral Column (Table 5). Many fundamental features of the camelid skeleton were established when the earliest North American camelids separated from other selenodont artiodactyls. For example, the vertebral formula has not changed since the Uintan (late middle Eocene), nor has the diagnostic feature of the cervical vertebrae, in which the vertebrarterial canal is concealed within the pedicles of the neural arch (Peterson, 1904). The long neck and gazelloid proportions already were clearly established in *Poebrotherium wilsoni* (Leidy, 1847), the common Oligocene camelid and the first fossil camelid known to science (Leidy, 1847, 1869). We show here that *C. gettyi* has more radically altered

its axial skeleton toward foreshortened proportions than any other known camelid.

Two articulated skeletons and two additional partial vertebral series provide all of the available evidence regarding the axial skeleton in this new genus (Table 5). Most importantly the holotype, LACM 124002, presents a virtually complete skeleton of a mature individual. The paratype, LACM 123978, provides most of the skeleton of an adolescent individual, although it lacks the cervical and anterior thoracic vertebral series. A third specimen, LACM 124001, represents the posterior portion of a mature skeleton from the sacrum back. Finally, LACM 145103 includes four lumbar vertebrae. The complete vertebral formula based on these specimens is C7 T12 L7 S5 Cd 10.

In the holotype skeleton the entire cervical series is articulated, as are the succeeding thoracic series and rib cage (Fig. 3). The cranium had broken loose from the atlas and lay about 18 mm lateral to it. The neck lay with a slightly upward and leftward arch, spanning a chord of 48.0 cm and placing the occipitoatlantal joint 48.0 cm anterior to the head of the left humerus. The measurements given in Table 5 approximate the original lengths of the vertebrae within about a 10% range of error as a result of distortion by crushing. In virtually all other camelids the axis is the longest vertebra, followed closely by the middle (third through fifth) cervicals. In C. *gettyi,* by contrast, the fourth and fifth cervicals are about the same length as the more posterior vertebrae. Clearly, this animal had a foreshortened cervical region, especially within the middle region where the necks of most camelids gain much of their length.

The atlas has powerful articulations for the occipital condyles, as expected in this relatively large-headed animal. The approximate dimensions of its deeply concave articular surface is 70.5 mm wide, 13.5 mm high, and about 20.5 mm in maximum anteroposterior depth. The axis is the longest vertebra, yet it is also broad and powerfully built. Its maximum width, measured across the anterior articular surface, is 76.7 mm. The dens is 14.0 mm long, 12.0 mm deep, and 24.0 mm wide, proportionally much wider than in extant camelids. The spinous process was evidently low in this and in all of the cervicals. The ventral crest is well developed in the posterior half of the atlas. It becomes progressively deeper and reaches farther anteriorly in each successive cervical. On the fifth cervical the posterior end of the ventral crest produces a deep tuberosity about 20 mm long and about 10 mm wide. The fifth cervical vertebra also has very broad zygapophyses, the posterior articular processes spanning about 59.3 mm. The sixth cervical has continuous ventral laminae that extend ventrolaterally at about a 45 degree angle from the vertical plane. They are about 71.5 mm long, slightly longer than the body of the vertebra, and about 12 mm deep. The ventral laminae spread broadly so that the distances between them are 93.5 mm anteriorly and 73.0 mm posteriorly. The structure of this sixth vertebra, with massive wings for insertion of the medioventral flexors of the neck (*M. longus colli*) is characteristic of camelids. Its features indicate that C. *gettyi* ordinarily carried its neck in a nearly vertical orientation and that the sixth cervical marked the locus of a nearly right-angle curve at the base of the neck as in other camelids.

The first thoracic vertebra in the holotype (LACM 124002) has large rib facets separated by a distance of just under 94 mm. The immature paratype skeleton, LACM 123978, presents two thoracic vertebrae. The thoracic spine on one is nearly complete and measures 51.5 mm in length. The widths across the rib articulations are 31.7 mm in both specimens.

A mature partial skeleton, LACM 145103, consists of four associated lumbar vertebrae. The second of these associated vertebrae is the best preserved, and its centrum measures 28.2 mm deep and 22.7 mm wide. In another mature partial skeleton, LACM 124001, the last lumbar vertebra has a posterior depth of 17.6 mm and a posterior width of 34.0 mm.

LACM 124001 also provides a sacrum associated with the last lumbar noted above. The anterior depth is 18.4 mm; the maximum width across the pelvic articulations is 80.9 mm, and the width across the anterior end of the neural canal is 24.9 mm. The dorsal portion of a fourth sacral vertebra is attached to the dorsal spinous region of the preceding two sacral vertebrae. All three have low neural spines with their sharper ends facing anteriorly. The fourth neural spine is about 12 mm wide at its base, whereas the more anterior ones are only about half of that dimension. LACM 123978, the immature paratype, also includes three sacral vertebrae. The anterior surfaces for pelvic articulation are strongly convex, slightly angled anteromedially, and deeply roughened for ligamentous attachments between the two bony surfaces. The pelvic articular face measures 42.3 mm deep and about 45 mm long. The first sacral foramen is 11.3 mm in diameter.

LACM 124001 provides ten caudal vertebrae, and these appear to represent the complete series. The neural arch and transverse processes on the first caudal vertebra were complete but are badly shattered. An element near the middle of the series, probably the fifth caudal, has a distinct transverse processes spanning a horizontal distance of 19.7 mm. Dorsally this vertebra bears a pair of minute mammilary processes that represent the vestigial walls of the neural canal. Equivalent dorsal morphology in a caudal vertebra of extant C. *dromedarius* occurs in about C8, but equivalent morphology with broad transverse processes would be found no farther back than about C4 in the extant species. The minute size of the probable tenth caudal vertebra in LACM 124001 suggests that it was probably the terminal element. In extant C. *dromedarius* the number of caudals varies between fif-

teen and twenty-one (Smuts and Bezuidenhout, 1987:20). Thus the caudal series in *C. gettyi* appears to be about two-thirds as long as in extant dromedaries but with the more powerful transverse processes near the middle of its tail.

Ribs and Sternum. As in camelids generally, the anterior part of the rib cage is extraordinarily narrow. The distance between the humeri, as registered in the articulated holotype skeleton (LACM 124002), measures 152.0 mm, and more posteriorly the maximum width of the rib cage is about 170 mm.

The sternum and associated ribs are preserved in their three-dimensional relationships in the juvenile paratype, LACM 123978. On the right side the sternal elements are seen to connect directly with the first seven ribs. The overall length of the sternum is 206 mm. Of the seven original sternebrae, the tiny first element is missing. The manubrium is about 57 mm long by 27 mm wide, proportionally wider and more massive than in extant *C. dromedarius* (see Smuts and Bezuidenhout, 1987). The entire sternum is bowed down ventrally so that the posterior end of the third element lies 20.0 mm ventral to an imaginary line from the manubrium to the xiphoid process. The fourth sternebra is about 50 mm wide and is thus the widest element. The fourth and fifth sternal elements each attain a dorsoventral thickness of 11.0 mm. They do not exhibit the extreme thickening, in which the depth of each sternebra nearly equals its width, that is associated in extant camelids with heavy sternal callosities upon which they rest. The sixth sternal element is fused with the seventh (xiphoid process); together they form the longest element with a length of 51.5 mm. The xiphoid process is wider and more trapezoidal than that of *C. dromedarius*, in which the posterior end is narrow and the overall shape subtriangular.

Scapula (Table 6). Both scapulae of the immature paratype skeleton, LACM 123978, are represented by their distal portions. In most of its features the scapula of *C. gettyi* resembles that of *Stenomylus* Peterson, 1906. The coracoid process is relatively narrow with a distinct concavity on its medial side. The acromion process is retracted proximally a considerable distance; it arises gradually from the main axis beginning some 35 mm above the glenoid fossa. It thus differs sharply from the powerful process that closely overhangs the glenoid in most later Cenozoic camelids. A large acromion foramen 3.0 mm in diameter lies about 10 mm anterodistally from the acromion process. The supraspinatus fossa is proportionally even smaller relative to the infraspinatus fossa than in progressive camelids. At the level of the scapular neck, the supraspinatus fossa is 8.0 mm wide, whereas the infraspinatus fossa is 23.0 mm wide. The thicker posterior border of the scapular neck bears two long vertical grooves for the origin of *M. triceps brachii*, that are more deeply pocketed than in *Stenomylus*.

Humerus (Figs. 10A–B; Table 6). The most notable feature of the humerus is its immense greater tuberosity that rises 33.0 mm above the head of the humerus. The greater tuberosity is wider (44.0 mm) than any other part of the humerus except the head and is 22.0 mm thick anteroposteriorly near midlength. The vast rugose area on the greater tuberosity provides an origin for *M. infraspinatus*. The head itself is very large and overhangs the shaft posterodorsally by nearly 20 mm. This overhang is proportionally about the same as in *Stenomylus* and much less streamlined than in progressive camelids. The proximal groove of the humerus is narrow and channelized by the magnitude of the other proximal features. The deltoid crest extends about 60 mm down the posterolateral side of the shaft. Distally the lateral epicondyle rises higher anteriorly and extends farther distally than the medial epicondyle. The olecranon fossa is deep and broad, a feature exaggerated in the immature specimen because it is incompletely ossified.

Table 6 Measurements of forelimb elements.

	LACM 123978 (mm)
Scapula	
Maximum distal length anteroposterior across coracoid	48.5
Maximum width across distal arm	27.5
Minimum anteroposterior diameter at neck	29.0
Height from arm to base of acromion	32.1
Humerus	
Overall length	229.1
Articular length	204.1
Maximum anteroposterior width across tuberosities	70.5
Maximum width across distal trochlea	46.5
Depth below medial epicondyle	37.2
Radius–ulna	
Overall length	261.1
Articular length	195.5
Maximum width proximal to articular surface	40.1
Width distal end	43.7

Radius and Ulna (Figs. 10C–D; Table 6). The olecranon process of the ulna has much longer and thicker proportions than that of *Stenomylus*. The portion that lies proximal to the main articular surface is 70.0 mm long and equals 28% of the functional length of the radius (196 mm). In *Stenomylus gracilis* Peterson, 1906, by contrast, the proximal portion equals 21% of the lower portion. Most more progressive camelids have even more elongate propodial proportions; for example, in *Camelops hesternus* (Leidy, 1854) this same relationship is 20%. The olecranon process in *C. gettyi* has a near-

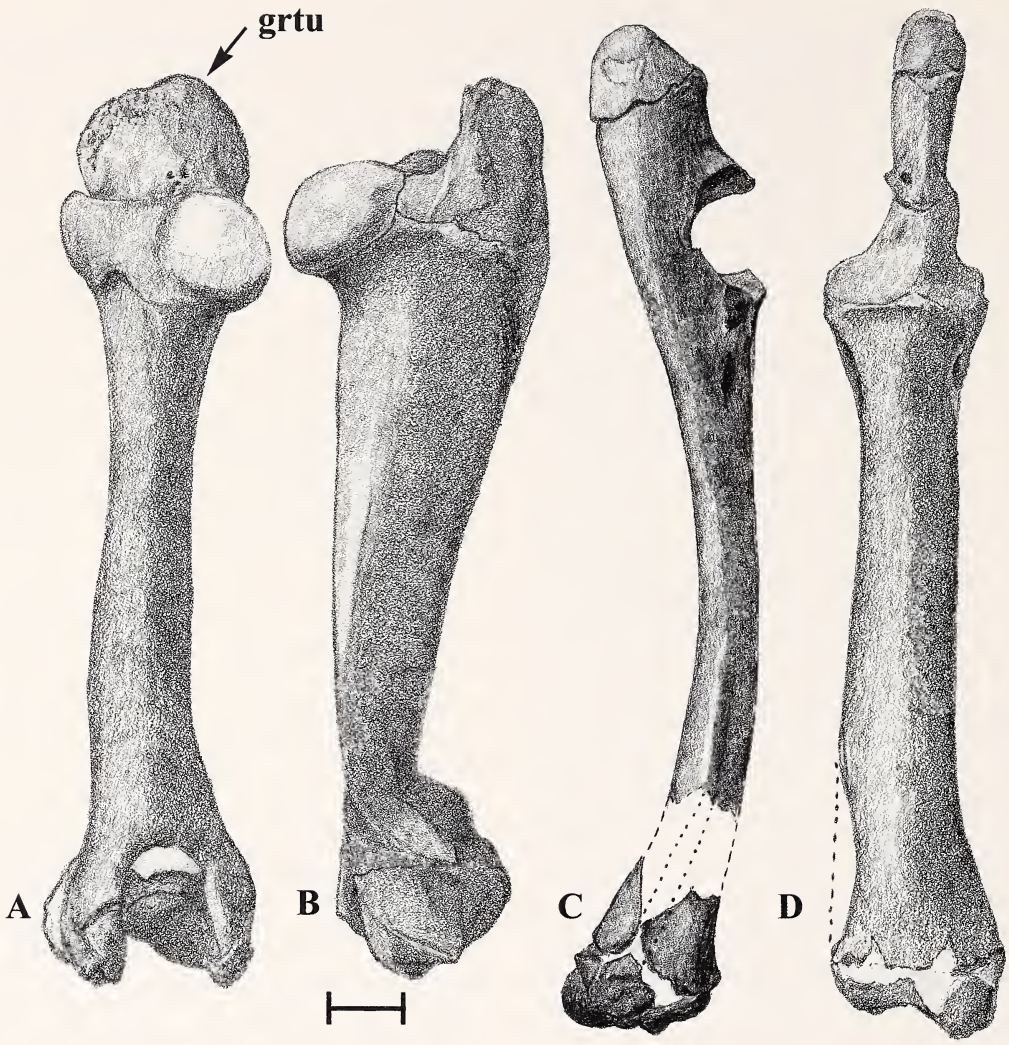

Figure 10 *Capricamelus gettyi,* juvenile paratype, R humerus, LACM 123978. A, posterior view; B, lateral view; C, R radius-ulna, lateral view; D, anterior view. Abbreviations: grtu = greater tuberosity. Scale bar = 1 cm

ly straight posterior profile, in strong contrast with the marked concavity of most camelids. On the lateral side the origin of *M. extensor digitalis lateralis* is marked by a prominent subrectangular tuberosity more than 10 mm on each side. The interosseous foramen just distal to this tuberosity is more than 12 mm long.

On the medial side of the radius a large triangular cavity extends from the sigmoid notch distally for a distance of about 21 mm. Its anteroposterior dimension near the proximal end is about 14 mm in the immature specimen. A similar feature appears in *S. gracilis* and was described as follows by Peterson (1908:292): "The radial border of the sigmoid notch is different from that in *Oxydactylus* and the recent camels in having an interrupted area in the deepest part of the notch". This area may provide the origin for medial collateral ligaments of the joint and also for the insertion of a powerful *M. biceps brachii.* As in other camelids, the styloid process of the ulna extends prominently into articulation with the cuneiform on the lateral side of the carpus. Here the distal ulna is poorly fused with the distal end of the radius; the distal ends are separated for about 60 mm on both sides of the immature specimen. The three distal facets for the carpus are nearly equal in width as in *Oxydactylus longipes* Peterson, 1904 (p. 455).

Carpus (Figs. 11A–C). The proximal carpal elements—scaphoid, lunar, and cuneiform—have saddle-shaped proximal surfaces with a considerable convexity near the anterior margin, indicating a powerful resistance to overflexion. The proximal dimensions of the whole carpus have a width about 30% greater than the anteroposterior depth. In LACM 123999, a mature articulated manus, the

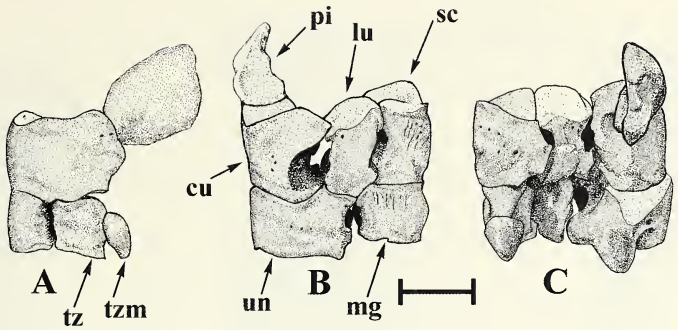

Figure 11 *Capricamelus gettyi,* adult referred specimen, R carpus, LACM 123999. A, medial view; B, anterior view; C, posterior view. **Abbreviations:** cu = cuneiform, lu = lunar, mg = magnum, pi = pisiform, sc = scaphoid, tz = trapezoid, tzm = trapezium, un = unciform. Scale bar = 1 cm

overall width is 48.8 mm, the medial depth is 34.9 mm, and the lateral depth is 37.6 mm. Unlike extant camelids, in which there is one large foramen between the scaphoid and lunar, here there are three large anterior openings lateral, medial, and distal to the lunar. The excavation of the lateral carpal opening is remarkable for its size which exceeds that on the anterolateral face of the scaphoid. A substantial trapezium, not ordinarily present in extant camelids, extends distally from its facet on the posterior face of the trapezoid. It is balanced laterally by a similar-sized palmar process of the unciform. The distal articular surfaces of the trapezoid, magnum and unciform are much flatter than in extant camelids, indicating very limited flexibility between the carpus and the proximal surfaces of the metacarpals.

Metacarpus (Figs. 12A–C; Table 7). Three unfused metacarpals are present in all but one of the articulated front feet. In LACM 124000, however, MC II is fused to the posteromedial face of MC III. MC II is a small, leaf-shaped bone about 15 mm long and 7 mm wide. Its articular surface faces the posteromedial margin of MC III and lies in a small pocket near its proximal end. MC III is usually about 2 mm longer than MC IV. Its proximal width averages 25.1 mm, whereas that of MC IV is 24.7 mm. The proximal ends of the two major metacarpals are closely appressed with rugose surface indicating that they were held in place by connective tissue. Two proximal facets on MC III mark an articulation between these two bones: the anterior facet is square, about 8 mm on a side, and faces distolaterally, thus resting on MC IV; the more posterior facet is subovate and measures 13.0 mm vertically and 9.0 mm anteroposteriorly. Near midlength the metacarpals become less closely connected, and their distal ends diverge as in other camelids. The distal ends of the metacarpals are substantially wider than the proximal ends. The median keel of each bone is confined to the palmar face as in other camelids.

Four pairs of large sesamoids are retained in their natural position in many of the front feet of *C. gettyi.* They lie with their long, slightly concave faces against the palmar faces of the metacarpals, one pair on each side of the median keel of each of the major metacarpals. They are involved in the ligamentous lacing of the fetlock joint, as can be inferred from Figure 12. Four pairs of ligamentous-attachments are well marked on the palmar faces of the metacarpals; they are flat subquadrate tuberosities about 10 mm wide by 15 mm long, just above the articular surfaces for the proximal phalanges. Those on the medial and lateral sides of each metacarpal represent the short sesamoid ligaments, and the pair on either side of the keel anchored the cruciate sesamoid ligaments. The four pairs of sesamoids and ligament sites were equally large on each of the metacarpals. Another important set of large ligaments are the collateral ligaments that run from the distal depressions on either side of each metacarpal to the proximal depressions and ridges on each side of each proximal phalanx. Finally, there was a powerful set of distal sesamoid ligaments that ran from each of the four pairs of sesamoids down the palmer face of each proximal phalanx. All of these elements of the fetlock joint capsule are extraordinarily well developed in *C. gettyi.*

Manual Phalanges (Figs. 12A–C; Table 8). The short, tightly bound phalanges of *C. gettyi* were posed in life in an unguligrade stance. This is reflected in the flat proximal and distal articulations of both proximal and medial phalanges. The two ranks of phalanges were closely bound together by interdigital ligaments at proximal, medial, and ungual levels.

The proximal phalanges are only about 50 mm long, and their thickness and depth equal about half of their length (see Table 8). As noted above, these proximal phalanges bear very deep fossae on their medial and lateral sides for powerful collateral ligaments. Another set of very large scars, representing an array of eight sesamoid ligaments, extend down about half of the palmar face of each

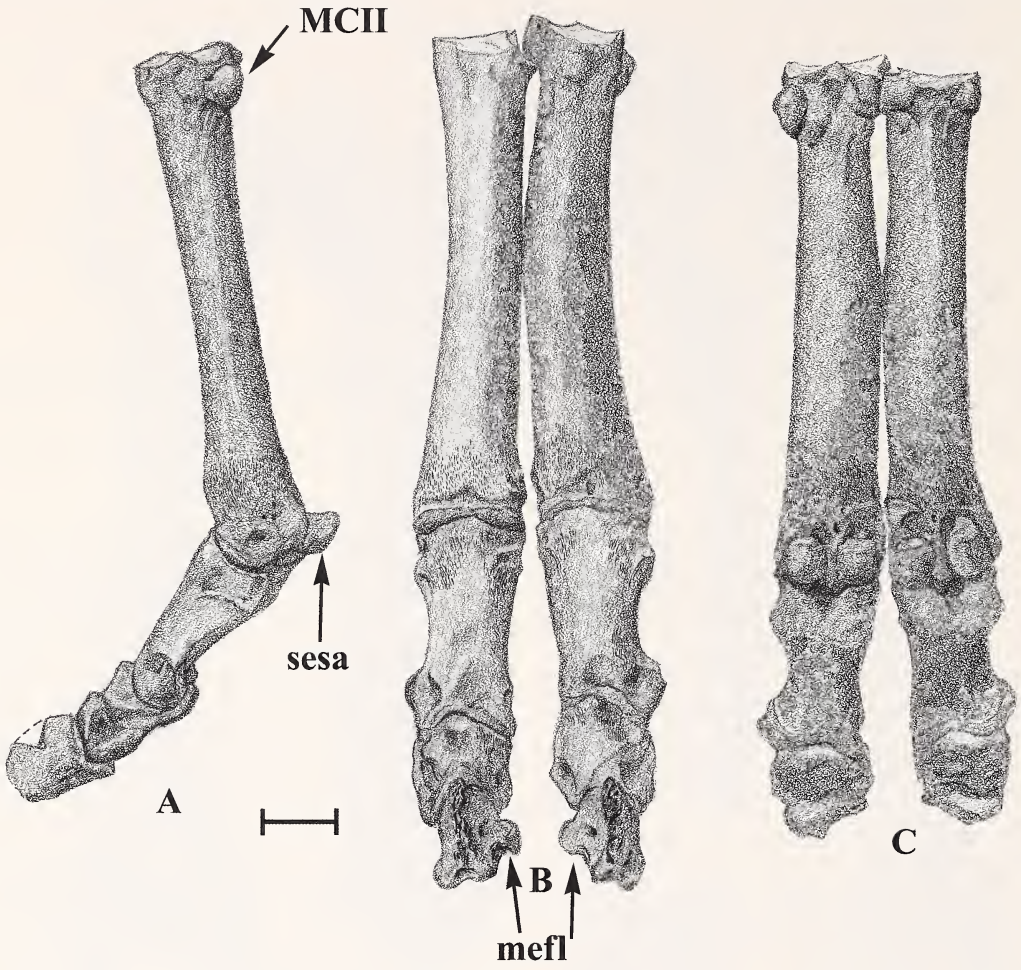

Figure 12 *Capricamelus gettyi,* adult referred specimen, R metacarpus and phalanges, LACM 123999. **A,** medial view; **B,** anterior view; **C,** posterior view. **Abbreviations:** MC II = second metacarpal, mefl = medial flange of ungula phalanx, sesa = large sesamoid on posteromedial side of MC III. Scale bar = 1 cm

proximal phalanx. This relationship of huge sesamoid bones to consistently powerful rugosities for their insertions are consistently represented in the many articulated feet of *C. gettyi.*

The ungual phalanges are extremely short and bear powerful medial flanges by which they were lashed tightly together with interdigital ligaments. The distal and plantar surfaces are pockmarked with numerous foramina, indicating that they were enveloped in well-vascularized connective tissue. Presumably that tissue was keratinized to form a compact pair of closely bound hooves, equivalent to the cloven hooves of a goat.

Pelvis (Table 9). The best preserved pelvis, the left side of LACM 124001, lacks only the anterolateral wing of the ilium. The delicate construction and narrow proportions of this element indicate a greater resemblance to the pelves of *Stenomylus* and *Oxydactylus* than to any more progressive camelids. This single best specimen of *C. gettyi* may represent a female individual, which would further account for its less massive features (Smuts and Bezuidenhout, 1987). The iliac crest extends anterodorsally in a long low arc, expanding gradually into a deep wing that faces laterally. The iliac wing measures at least 84 mm wide in this specimen; it surely would be considerably broader in the area of the tuber coxae, were that preserved. The thickness of the ilium ranges from less than 10 mm to more than 12 mm and is faintly concave on the broad lateral surface where the *M. gluteus* complex takes its origin. On the medial face the features associated with the sacral articulation are obscured by minor breakage. The corpus of the ilium narrows to a minimum depth of 37 mm and thickens transversely to a minimum of 18 mm. The dorsal and ventral margins are gently concave.

The width of the pelvis from acetabulum to pubic symphysis is 103.0 mm. On the medial side of the ilium, a strong ridge for the origin of *M. psoas* ex-

Table 7 Measurements of metacarpals.

LACM	Measure (mm)									
	122333	123964	123965	123966	123967	123972	123973	123999	124000	124002	Mean
Metacarpal III											
Length	144.4	138.3	—	137.6	132.0	143.1	146.0	135.5	134.8	135.7	138.6
Proximal width	26.3	25.8	—	26.9	23.5	24.3	22.8	24.5	27.8	24.2	25.1
Proximal depth (anteroposterior)	29.0	28.3	—	28.1	24.9	24.6	26.9	27.0	29.0	26.1	27.1
Distal width	28.4	30.8	29.4	31.0	—	30.1	30.0	29.2	31.9	30.9	30.2
Metacarpal IV											
Length	142.4	134.2	143.5	135.5	128.7	141.0	139.6	133.5	130.1	131.5	136.0
Proximal width	24.6	25.5	24.5	25.7	—	—	23.4	24.3	25.9	23.9	24.7
Proximal depth (anteroposterior)	26.7	27.2	26.2	27.5	27.0	26.4	25.8	27.9	28.0	26.4	26.9
Distal width	27.9	29.9(a)	28.7	29.2	27.4	29.6	28.2	29.8	28.5	27.6	28.7

tends about 25 mm, where it gives way to a sharp ridge that makes a large arc medially. Just over 20 mm anterior to the acetabulum is the tuberosity for the origin of *M. rectus femoris.*

The pubic symphysis is unfused in this mature specimen. It attains its maximum thickness, 18.3 mm, in its anterior third. The length of the pubic symphysis, as preserved, is 67.3 mm and is probably missing only a few more millimeters of thin bone from its posterior end. The transversely oriented neck of the pubis is 23.8 mm wide and 14.9 mm thick.

The fissure on the medial side of the acetabulum was evidently wide, but the specimen is badly broken. The thyroid fenestra is oval. The ischium extends nearly 103 mm to the well-developed sacral tuberosities. It narrows to a width of 26.1 mm at the concavity on its dorsomedial surface. A posteromedial buttress 80.0 mm long supports the sacrum. At the more lateral of two tuberosities on this sacral surface the ischium reaches a thickness of 21.7 mm, its maximum diameter.

Femur (Figs. 13A–B; Table 9). The proximal end of the femur is adequately represented only by the left side of LACM 124001. Fortunately several other specimens provide a fuller indication of the middle and distal part of this element. The head is set off medially on a proportionally longer neck than in extant camelids. The greater trochanter is remarkably well developed. It rises 12.0 mm above the level of the femur head, in contrast with extant camelids, in which the head is higher than the greater trochanter. It measures 34.0 mm anteroposteriorly and is notable for its rugosity on both its lateral and anterior faces. The trochanteric fossa is deep and expanded transversely to a width of about 30 mm. The lesser trochanter lies nearly 30 mm posteromedial to the femur head giving further definition to its neck. In *C. gettyi* the lesser trochanter extends 17 mm posterior to the posterior wall of the femur and forms a tuberosity more than 12 mm thick. This trochanter is far more prominent than in extant camelids; rather it is broadly comparable to the enlarged "knob" of *Oxydactylus* and *Stenomylus* (Peterson, 1904:462).

In posterior view, the lesser trochanter forms a prominent medial wing running down the proximal end of the femur. It extends distally 45 mm before it subsides to a modest longitudinal muscle scar, the linea aspera also evident in extant camelids. Distally this scar connects centrally with a tuberculated ridge that represents the origin of *M. supracondylaris lateralis.*

In caudal aspect three additional features appear toward the distal end of the femur. A massive strip of rugosities, up to 12 mm wide, extends down the lateral margin from 50.0 to 20.0 mm above the lateral condyle. This represents the lateral head of a powerful *M. gastrocnemius,* which functions to extend the hind foot by drawing up the tubanterolaterous head of the calcaneum. Near the medial side at about the same level is a low rugosity for

Table 8 Measurements of digit III, manual phalanges.

	Measure (mm)												
LACM	122333	123964	123965	123966	123967	123972	123973	123974	123975	123978	123999	124000	124002
Proximal phalanx III													
Length	48.5	49.9	52.3	48.5	48.5	53.2	53.2	45.7	47.5	50.4	51.0	48.4	46.2
Proximal width	29.1	29.2	28.0	27.4	25.4	25.8	30.0	25.7	26.1	24.6	25.5	27.6	27.0
Proximal depth	24.3	24.8	26.6	23.7	22.3	22.4	23.7	22.3	22.5	22.0	23.0	24.3	24.8
Distal width	24.1	25.5	24.4	24.9	23.1	23.8	25.1	23.4	23.7	20.1	25.3	25.6	23.9
Medial phalanx III													
Length	32.4	31.9	33.3	31.6	28.4	30.3	30.6	29.8	31.0	26.5	29.9	29.3	31.4
Proximal width	23.6	24.0	23.2	23.7	22.7	23.3	21.7	23.2	23.1	20.3	24.3	23.6	23.4
Proximal depth	21.0	19.9	20.1	20.1	19.5	18.7	20.3	19.9	19.3	19.6	19.9	20.1	19.8
Distal width	22.9	24.4	23.1	23.9	22.3	23.6	21.9	22.2	22.5	19.8	24.4	24.2	23.2
Ungual phalanx III													
Length	27.0	28.9	—	—	26.1	26.2	—	26.2	25.8	26.1	25.3	26.4	26.1
Proximal width	20.9	19.8	—	20.0	18.5	19.6	—	21.5	22.6	14.1	19.0	18.9	20.2
Proximal depth	20.2	20.8	—	19.8	18.8	18.9	—	17.1	18.1	17.2	18.9	19.9	18.4
Distal width	11.0	11.4	—	11.4	10.3	11.5	—	11.1	11.1	10.6	10.6	11.4	9.6

Table 9 Measurements of hind limb elements.

	Measure (mm)	
	LACM 124001	LACM 124002
Pelvis		
Greatest length of pelvis	314.0 (estimated)	
Corpus of ilium	37.0	
Diameter of acetabulum	40.0	
Transverse length of ischium	103.0	
Width of pelvis across	103.0	
Length of pubic symphysis	67.3	
Long-diameter thyroid fenestra	66.0	
Femur		
Greatest length	274.0	292.0
Functional length	262.0	280.0
Transverse diameter proximal end	87.9	97.6
Diameter midshaft	28.6	31.8
Distal width	62.1	58.7
Distolateral depth	61.9	57.6
Patella		
Length	64.3	57.8
Maximum proximal width	40.0	45.4
Maximum thickness	27.5	25.9
Maximum distal width	35.5	34.4
Tibia		
Length	274.0	283.0
Proximal width	64.5	61.6
Distal width	48.1	47.6
Distal anteroposterior	28.2	26.3
Fibula		
Height (including shaft)	21.6	20.4
Anteroposterior diameter	25.3	23.6
Transverse diameter	14.4	13.4

M. flexor digitalis superficialis. Finally, there is an extremely prominent tubercle about 12 mm dorsomedial to the medial condyle, which evidently marks the origin of an unusually large medial collateral ligament (Smuts and Bezuidenhout, 1987: 55).

The femoral condyles appear large relative to the shaft diameter. They are slightly oblique, as in other camelids, with a lateral twist. The lateral condyle has a larger diameter than the medial. The intercondyloid fossa has three subdivisions from which the cruciate ligaments of the knee joint arise. The deep triangular notch lateral to the trochlear groove houses the *M. popliteus* as in all camelids. The patellar groove is exceedingly wide (31.5 mm) and deep (7.2 mm), with the lateral margin higher than the medial margins.

Patella (Figs. 13C–D; Table 9). The patellae are quite variable in shape, but they are all roughly trapezoidal with a long dorsoventral diameter and the proximal width greater than the distal width. Both medial and lateral sides are concave. The cranial aspect is strongly convex and deeply rugose. The caudal face of the patella consists of two elongate articular faces with a gentle ridge smoothly dividing them. The lateral articular surface is longer and extends farther proximally than the medial. In comparison with extant camelids, this patella is proportionally wider, distally more blunt, and much more convex on the articular surface.

Tibia (Figs. 14A–C; Table 9).

The tibia is the longest bone in the skeleton of *C. gettyi*. The triangular proximal end is much more massive than the anteroposteriorly compressed distal end. Proximally the medial condylar facet is more concave and subovate, whereas the lateral facet is saddle shaped with considerable anteroposterior convexity and extends posterolaterally well beyond the tibial shaft. This lateral facet terminates at the fused proximal vestige of the fibula. Of the two intercondylar tuberculi near the middle of the proximal end, the medial tubercle is slightly taller and is placed more anteriorly than the lateral tubercle. The cnemial crest is about 40 mm long and is disproportionately wide compared with the overall width of the tibia. In *C. gettyi* its width is 46%, compared with 38% in extant *C. dromedarius*. The anterolateral sulcus for the extensor ligament forms a relatively large excavation which spans nearly 12 mm along the perimeter of the bone and also forms a notch an equal distance toward the center of the proximal surface. Midway along the posterior face of the tibia a rugosity about 40 mm in diameter overhangs the posterior concave area and serves as the attachment site for the caudal cruciate ligaments.

The distal end of the tibia is notable for the great distal extent of its medial malleolus. This malleolus is 8.3 mm wide and about 13 mm long anteroposteriorly. Its medial face is rugose and heavily invested with ligaments and fasciae. The transverse dimension is about 78% greater than the maximum anteroposterior dimension, whereas in *C. dromedarius* that percentage is about 61%, and in *C. hesternus* it is about 68%. The notch for the lateral mallelus is broader and shorter than in extant camelids and also proportionally shorter than in *Stenomylus*.

Fibula (Figs. 15A,C; Table 9). The distal remnant of the fibula has an unusually blunt shaft. It rises only about 5 mm above the distal articulation and therefore has no deep recess on the lateral surface of that bone. The two proximal facets for the tibia are about 9 mm wide and meet smoothly along a steep divide that separates the smaller anterior from the larger posterior facet. The medially facing as-

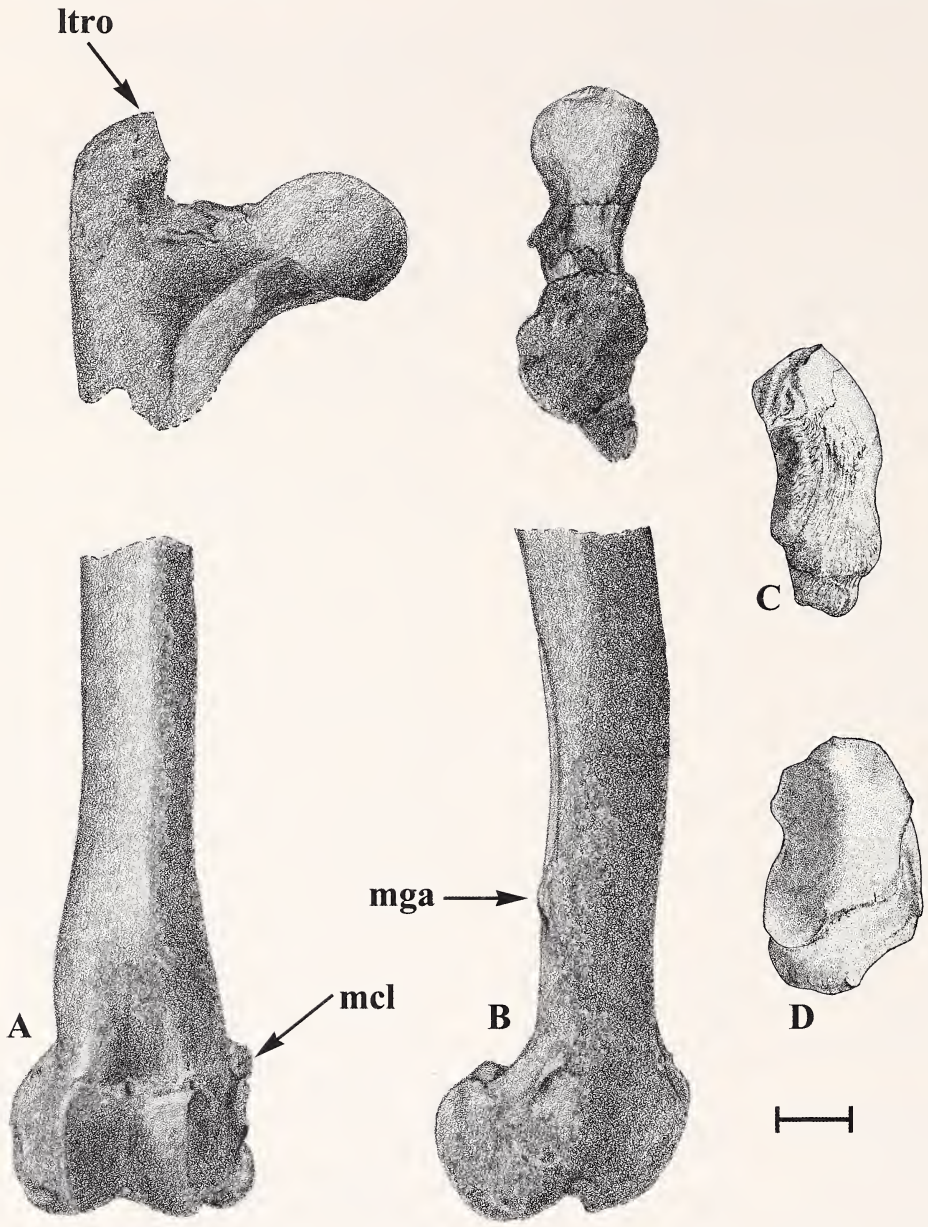

Figure 13 *Capricamelus gettyi,* adult referred specimen, R femur, LACM 124001. A, anterior view; B, lateral view; C, R patella, lateral view; D, posterior view. **Abbreviations:** ltro = lesser trochanter, mga = scar for *M. gastrocnemius,* mel = scar for medial collateral ligament. Scale bar = 1 cm

tragalar facet is gently convex in two dimensions. Its proximal margin is a well-defined semicircular rim which rides on the lateral trochlea of the astragalus. The distal surface of the fibula is sharply divided into a large posterior concavity for the parasustentacular surface of the calcaneum and a much smaller anterior concavity that locks into the distal convexity on the calcaneum during extreme pedal extension.

Tarsus (Figs. 15A–C). The tarsus consists of six bones, the astragalus and calcaneum proximally and the entocuneiform, ectomesocuneiform, navicular, and cuboid in the more distal row. In a functional sense, one can also include a seventh element in the proximal row, the vestige of the distal fibula, also known as the lateral malleolus. The height of the tarsus is about 55 mm, measured from the lateral crest of the proximal trochlea of the astragalus to the distal end of the cuboid, and this is half of the metatarsal length. Furthermore, if one incorporates the extended calcaneum to give the functional length of the tarsus, then, quite remarkably,

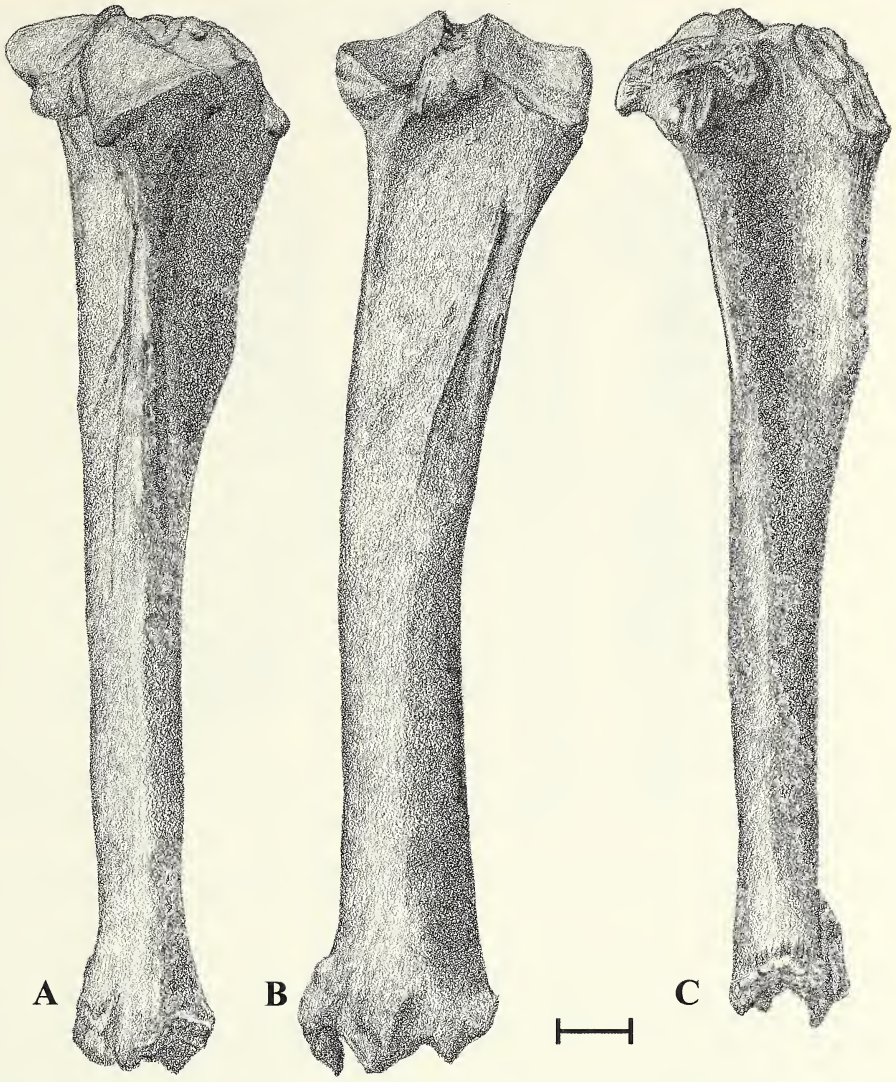

Figure 14 *Capricamelus gettyi,* adult referred specimen, R tibia, LACM 124001. **A,** oblique lateral view; **B,** posterior view; **C,** lateral view. Scale bar = 1 cm

the tarsus length equals the metatarsus length in *C. gettyi.*

Astragalus (Figs. 15D–F). The astragalus of *C. gettyi* is remarkably short and broad. The two prominent ridges of the proximal trochlea are sagitally oriented, even at their plantar ends. The lateral ridge reaches more proximally than the medial. The lateral fibular facet is deeply excavated. The sustentacular facet is concave transversely and, as in *Miolabis* its medial portion overhangs the body of the astragalus and makes contact with the small vertical facet on the medial side of the calcaneum. The medial side of the distal trochlea is notable for the very deep stop facets on its anterior and posterior faces. Evidently these features worked to block either overextension or overflexion. In *Miolabis fissidens* Cope, 1876, only the posterior stop facet is well developed.

Calcaneum (Figs. 15A–C). The corpus of the calcaneum in LACM 124001 is 26.0 mm long, while the tuber calcis measures about 60 mm. Thus the corpus in *C. gettyi* appears relatively short compared with the tuber calcis. This contrasts with the calcaneal proportions in *Stenomylus* where the corpus makes up the greater part of the calcaneal length. The lateral wall of the corpus calcanei is not as deeply concave as in *Stenomylus.* The cuboid facet is nearly rectangular and unusually long, measuring about 12 mm by 20 mm. It is somewhat broader at the anterodistal end. The sustentacular facet is 20.0 mm wide and is the largest of the three distal facets. On the medial side there is a small

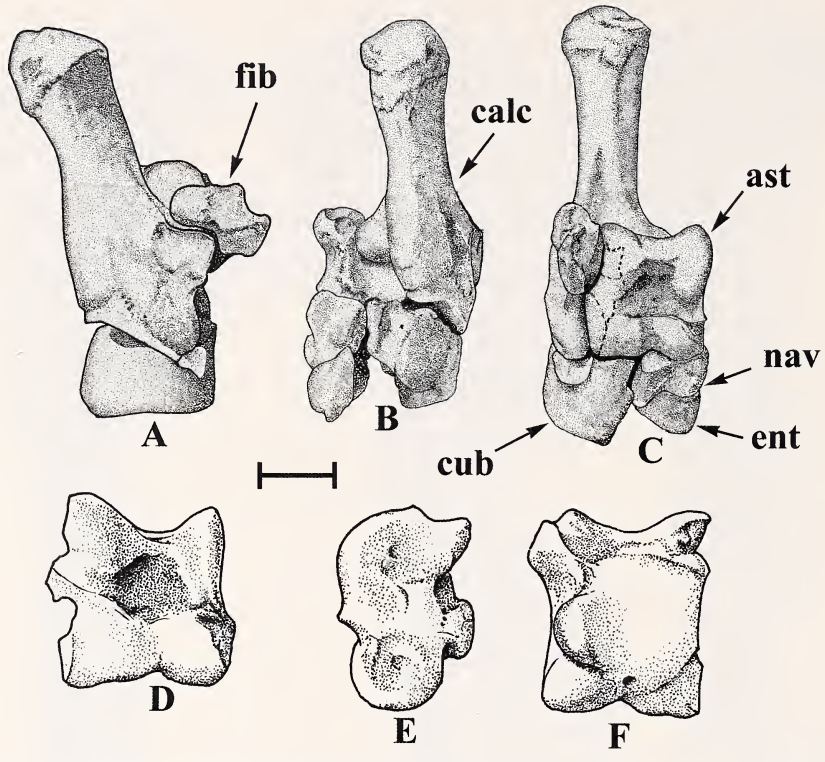

Figure 15 *Capricamelus gettyi*, adult referred specimens. A–C, R tarsus, LACM 124002: A, lateral view; B, posterior view; C, anterior view. D–F, R astragalus, LACM 124001: D, anterior view; E, lateral view, F, posterior view. **Abbreviations:** ast = astragalus, calc = calcaneum, cub = cuboid, ent = entocuneiform, fib = distal remnant of fibula, nav = navicular. Scale bar = 1 cm

vertical facet distinct from the main sustentacular facet. The same distinct medial sustentacular facet occurs in *Miolabis fissidens*. The parasustentacular facet in *C. gettyi* is saddle shaped with the concavity running proximodistally and the broad convexity extending from the deep lateral portion to the shallow medial portion. The second parasustentacular facet seen in most camelids is absent in all examples of *C. gettyi*. It is also missing from all calcanea we have seen of *Poebrotherium* and *Miolabis*.

Navicular (Figs. 15A–C). As in other camelids the navicular is separate from the cuboid, although it is closely appressed to it along a broad lateral surface marked by four broad facets. The proximal surface presents a deep concavity for the distomedial trochlea of the astragalus. A smaller anterolateral concavity receives the medial ridge of the astragalus. Distally a large ovate facet articulates with the ectomesocuneiform. It extends posteromedially and, without any break, meets the much smaller entocuneiform. Finally, at a slightly more distal position on the posteromedial face is a slightly convex subrectangular facet for MT II.

Cuboid (Figs. 15A–C). The proximal surface of the cuboid is divided into two subequal, but very different, surfaces. The medial concavity is congruent with the large concavity of the navicular and it receives the distolateral trochlea of the astragalus. Laterally a long plane surface slopes distally toward its anterior end. In LACM 124001 this facet is 9.9 mm wide anteriorly and 11.1 mm wide posteriorly. Its sloped anterior end notches the otherwise thick cubic structure of the cuboid and locks against the distal facet of the sustentaculum, thus helping the calcaneum to rotate the foot around the astragalar trochleae. Distally a very large semicircular facet articulates with the corresponding facet of MT IV. Posteriorly a smaller, transversely oriented facet meets MT II.

Entocuneiform (Figs. 15A–C). In LACM 124001 this small element measures 14.4 mm anteroposteriorly, 7.9 mm transversely, and 22.0 mm in height. Thus, it is taller than in an extant *Camelus*, but otherwise very small. It has three ovate facets: a proximal concave facet for the navicular, a lateral facet which meets the ectomesocuneiform, and a distal posteromedially facing facet for MT II. The entocuneiform does not meet MT III as in extant camelids.

Ectomesocuneiform (Figs. 15A–C). This larger bone is only 10.6 mm deep. Proximally it has a long oblique facet that is slightly concave anterolaterally and slightly convex posteromedially. It is

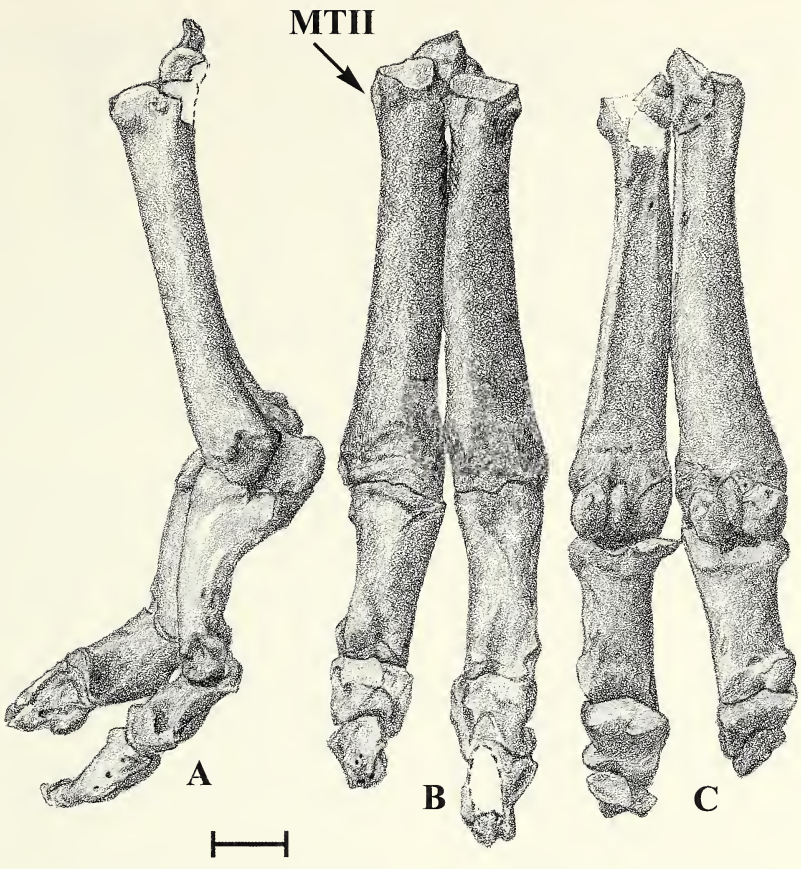

Figure 16 *Capricamelus gettyi,* adult referred specimen, L metatarsus and phalanges, LACM 124002. **A,** lateral view; **B,** anterior view; **C,** posterior view. **Abbreviation:** MT II = remnant of second metatarsal. Scale bar = 1 cm

ovate with a long diameter of 20.0 mm in LCM 124001. Near its anterolateral edge this bone produces a nearly vertical ovate facet that meets the cuboid laterally. Distally, a large flat facet corresponds to the proximal surface of MT III and reaches onto the large plantar process of that metatarsal.

Metatarsals (Figs. 16A–C; Table 10). The presence of MT II is indicated regularly by a pocket on the proximomedial side of MT III, which measures about 11 mm long and 7 mm wide. In the articulated hind foot of LACM 124001, MT II is fully preserved. It measures 18.2 mm long, extending down the posterolateral face of MT III. Its proximal facet, which articulates with the posteromedial facet of the entocuneiform, is lightly concave and measures 9.6 mm long by 7.7 mm wide. There are two subcircular facets, each about 6.5 mm in diameter, near the distal end of MT II. One faces distomedially and occupies a pocket in the plantar process of MT III. The other lies more distolaterally and faces almost directly anterior on the posterolateral surface of MT III. This arrangement of facets indicates that MT II retained some flexibility and had an autonomous set of ligaments to hold it during pedal movements.

The two major metatarsals are shorter and more lightly constructed than the metacarpals. As with the forefeet, these metatarsals are completely unfused in every individual. In LACM 123969, a mature individual, the proximal width of the two appressed metatarsals is 38.3 mm and their length is about 113 mm. The distal width across the two metatarsals is 49.0 mm. There are two proximal facets by which MT IV supports MT III. They resemble the two sets of metacarpal facets, except that the anterior facets do not overlap as widely in the metatarsals. The plantar process of each of the two major metatarsals is long and reaches proximally above the articular surface. On the proximal surface of MT IV the cuboid facet faces dorsolaterally and measures 7.0 mm anteroposteriorly and nearly 20 mm transversely. The proximal facet of MT III, for the ectomesocuneiform, faces dorsomedially and is quadrate in outline, measuring about 10 mm on each side. Together the proximal surfaces of the metatarsals are considerably deeper than wide, whereas in the smaller *Poebrotherium*

Table 10 Measurements of metatarsals.

	Measure (mm)							
LACM	27477	27479	27481	123968	123969	123978	124004	124002	Mean
Metatarsal III									
Length	113.6	121.8	121.9	114.6	113.2	—	112.1	112.3	115.6
Proximal width	20.4	20.4	20.6	21.0	20.7	—	23.0	20.3	20.9
Proximal depth (including plantar process)	28.6	—	28.2	27.9	28.7	—	—	28.2	28.3
Distal width	25.6	26.0	27.0	25.2	25.7	26.3	26.1	25.9	26.0
Metatarsal IV									
Length	115.8	125.9	125.2	115.1	116.7	111.4	114.2	114.5	117.4
Proximal width	20.4	19.9	20.7	19.6	20.8	19.6	21.2	19.4	20.2
Proximal depth (including plantar process)	28.8	29.4	30.6	28.3	27.9	28.7	—	30.4	29.2
Distal width	23.9	26.3	25.4	24.9	24.3	23.6	25.4	26.1	25.0

Figure 17 *Capricamelus gettyi,* referred specimen from Smith Creek Cave, Nevada, Nevada State Museum number 26WP46/45, proximal end, L metatarsus III. Scale bar = 1 cm

they are wider than deep. The distal tuberosities for the ligaments of the fetlock joint are much less developed than those in the forelimb.

A fully articulated left pes (LACM 27481) provides an interesting view of the foot in a flexed position. It exemplifies the way in which the deep surfaces of the cuboid and navicular engage the distal trochlea of the astragalus as its proximal trochlea is fully locked into the distal cochlea of the tibia. At that fully flexed stage the tuber of the calcaneum and the rest of the foot lie in the same plane as it makes nearly a right angle with the tibia. The tarsus including the tuber is nearly 90% as long as the metatarsus (109.8 mm vs. 123.4 mm).

Pedal Phalanges (Figs. 16A–C; Table 11). The medial and ungual phalanges are foreshortened in a similar fashion to the manual phalanges. The ungual phalanges bear opposing flanges similar to those in the manual ungual phalanges.

Body Proportions. The head of *C. gettyi* is unusually large for its body size, and this tendency is emphasized by the massively expanded cheek region (Fig. 9). The rostral region of the cranium is deep and extraordinarily robust, in connection with the powerful viselike occlusion of its enlarged upper and lower incisors. With regard to this anterior portion of its cranium, *C. gettyi* more nearly resembles a grazing equid than any other camelid.

The neck region of *C. gettyi* differs considerably from that of any other camelid in its foreshortened proportions. The atlas, as in all known camelids, is the shortest cervical, presumably because its primary function is to support the head via the occipital condyles. We may therefore take the atlas as a relative measure of length for the other cervicals. In *L. guanicoe,* the atlas is about the same length as that of *C. gettyi,* but the whole cervical series is about 20% shorter in *C. gettyi* (503 mm) than in *L. guanicoe* (620 mm). In most camelids the longest vertebrae are the axis and the intermediate cervicals (C3 through C5), and they are usually 250 to 300% longer than the atlas. In *C. gettyi,* likewise, the axis and the next three vertebrae are the longest vertebrae, but they are only 40 to 50% longer than the atlas. In *C. gettyi* each of the five vertebrae be-

Table 11 Measurements of digit III pedal phalanges.

	Measure (mm)										
LACM	27477	27479	27481	123968	123969	123970	123971	123977	123978	124001	124002
Proximal phalanx											
Length	48.5	50.3	50.9	50.3	45.9	51.0	51.5	45.7	48.9	48.1	47.1
Proximal width	22.6	22.5	24.5	24.2	25.9	23.5	—	24.3	25.2	24.8	23.4
Proximal depth	20.2	22.6	22.2	27.2	21.1	21.4	—	24.3	21.1	21.8	23.3
Distal width	19.0	20.0	19.1	18.6	20.2	18.4	19.2	22.4	19.8	20.2	19.7
Media phalanx											
Length	29.2	30.4	31.0	30.5	30.3	29.6	29.6	28.6	27.9	29.3	28.3
Proximal width	20.3	21.2	19.8	21.0	21.4	20.4	21.3	20.7	22.5	22.2	21.7
Proximal length	18.5	19.0	18.2	—	18.9	19.1	18.7	18.3	19.7	22.0	—
Distal width	19.3	20.2	20.7	20.2	19.7	20.4	20.1	20.5	17.8	20.9	21.6
Ungual phalanx											
Length	31.2	27.6	26.9	25.7	32.6	26.6	27.8	23.9	27.1	33.8	28.3
Proximal width	15.6	16.3	15.9	17.0	16.1	16.6	16.5	17.3	14.5	16.6	17.0
Proximal depth	19.5	18.9	19.0	17.6	19.9	19.1	19.2	16.4	17.2	20.1	16.8
Distal width	10.0	9.2	8.9	9.0	9.7	9.1	9.2	9.1	9.2	10.1	9.0

tween the first and last cervicals is at least 20 cm shorter than its counterpart in *L. guanicoe,* thus resulting in a neck length that is about 20% shorter than in a more typically proportioned camelid.

The tail may also have been shorter and somewhat more heavily built in *C. gettyi* than in most camelids. It consists in one specimen of only ten caudals, and the middle caudals have unusually broad transverse processes.

The body posture is partly indicated by the resting position of the articulated holotype skeleton (Fig. 3). In this specimen the humeri are horizontally disposed along both sides of the rib cage, and the radii stand essentially vertically. Presumably these relationships represent normal standing posture.

REFERRED SPECIMENS. We briefly note two specimens that add importantly to the chronological and geographic range of *Capricamelus.* One from Smith Creek Cave in Utah, in the collection of the Nevada State Museum, numbered 26WP46/45, collected from a pinkish silt stratum, represents the proximal end of the left MT III (Fig. 17) (Miller, 1979). It compares in detail with other unfused elements of this same nature in the type locality of *C. gettyi.* The proximal dimensions are 25.6 mm anteroposteriorly across the plantar process and 18.5 mm in transverse diameter.

This Utah record should not be confused with *Oreamnos herringtoni* Stock, 1936 (type and other material), from Smith Creek Cave in Nevada (Stock, 1936). The paratypes of that species are fully fused front and hind cannon bones. Although they are proportionally similar to the metapodials of *Capricamelus,* their detailed morphology is clearly bovid, not camelid.

A proximal phalanx from Mormon Mesa in Clark County, Nevada, catalogued in the collections of the AMNH as F:AM 108533 measures 50.0 mm long; the proximal dimensions are 22.7 mm deep, 25.5 mm wide, and 24.0 mm in anteroposterior diameter. Its distal dimensions are 13.0, 17.5, and 13.6 mm respectively. The morphology and measurements are closely comparable to those of proximal phalanges of *C. gettyi.* Unfortunately nothing is known regarding the age of this isolated Nevada specimen. The exact locality is indicated in Ted Galusha's 1963 field notes at the Frick collection of the AMNH.

PHYLOGENETIC RELATIONSHIPS

Capricamelus gettyi presents a bewildering array of primitive and uniquely specialized characters. For many years after its original collection there was even some question as to whether it was a camelid. This concern was heightened by the skewed morphological sample from the Tecopa Lake Basin in which the goatlike limb proportions and tightly bound feet were more fully evident in *C. gettyi* than its craniodental anatomy. In the following discussion we first place this new genus and species phylogenetically within the family Camelidae, and then broadly within the subfamily Miolabinae, also suggesting close affiliation with the probable sister subfamily Stenomylinae. Third, we indicate why Capricamelus is a the most derived genus hitherto recognized within the subfamily Miolabinae.

The following set of derived characters clearly reflect an ancestry uniquely shared with other Camelidae.

1) Mastoid bone broadly exposed in posterolateral region of cranium
2) Cancellous auditory bulla composed of two ventrally extended plates separated posterolaterally by a deep tympanohyal recess

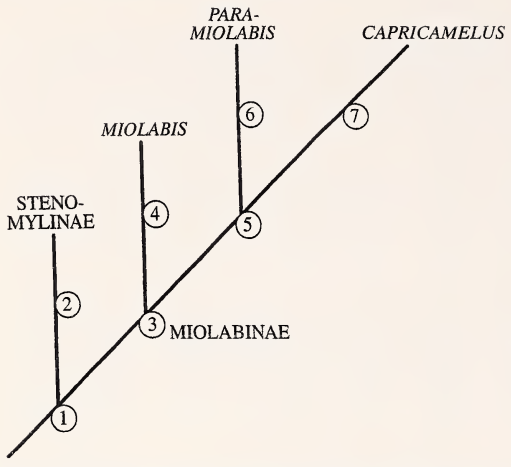

Figure 18 Relationships of the genus *Capricamelus* within the camelid subfamily Miolabinae. Key to characters at the numbered nodes. Node 1, enlarged I^1 and I^2 occluding in transverse arcade with lower incisors; elongate rostrum; premaxillary bone wedges posteriorly between nasal and maxillary; closed orbit with broad postorbital bar; auditory bullae transversely compressed; mandible lacks posterior mental foramen; mandible with expanded posteroventral apron; angular hook reduced or absent; short coronoid process. Node 2, partially fused metapodials; mesostyles lost. Node 3, parastyles reduced on P^2 and P^3; cervical vertebrae abbreviated; metapodials short. Node 4, I^1 and I^2 cupped; P_1 absent. Node 5, more elongate rostrum with long upper and lower diastemata; extremely compressed bullae; P^2 absent; P^3 greatly reduced; P^4 reduced; P_2 vestigial or absent; P_3 greatly reduced; P_4 reduced; cheek teeth more hypsodont; upper molars with flattened labial ribs and styles; lower molars with flattened lingual walls and weak stylids. Node 6, lower molars with anterior buttresses. Node 7, greatly enlarged incisors; very long diastemata with loss of P^3 and P_3; greatly increased hypsodonty, very short metapodials

3) Parietal portion of cranium longer than frontal
4) Postglenoid process articulating anteriorly with facet of mandibular condyle
5) Mandibular symphysis solidly fused
6) Six cervical vertebrae conceal vertebrarterial canal within neural arch
7) Fusion of the ectocuneiform with the mesocuneiform in the pes
8) Metapodials with distal keels confined to the plantar surfaces
9) Distal (coffin joint) sesamoids cartilaginous, not ossified

In addition, we note the absence of two features that would be expected in Ruminantia but not in Camelidae, namely horns or antlers and fusion of the cuboid and navicular in the pes.

Within the Camelidae, *C. gettyi* can be assigned to the subfamily Miolabinae (Fig. 18, Node 3). This new taxon shares the following derived features with other members of that subfamily.

1) Enlarged upper I^1 and I^2
2) Elongate rostrum with maximum width across incisors
3) Bulla deep and narrowly compressed
4) Mandible with expanded posteroventral apron
5) Angular hook reduced or absent; coronoid process short

One other phylogenetic implication of our study is that the subfamily Stenomylinae is probably the sister group of the subfamily Miolabinae. The subfamily Stenomylinae has been well studied during the past century. Classic work on the primitive genus, *Stenomylus,* by Peterson (1906, 1908) was augmented by Frick's (1937) description of *Rakomylus* and culminated in a full review of the subfamily (including description of a third genus, *Blickomylus)* by Frick and Taylor (1968). Shared–derived features that indicate the sister group relationship of Stenomylinae with Miolabinae include the following.

1) Enlarged I^1 and I^2 occluding in a transverse arcade with lower incisors
2) Elongate rostrum, with tendency to reduce intermediate premolars
3) Premaxillary bone elongate, wedging posteriorly between nasal and maxillary bones
4) Postorbital bar very broad
5) Auditory bullae tending toward transverse compression
6) Mandible lacking posterior mental foramen
7) Mandible with expanded posteroventral apron
8) Short coronoid process
9) Angular hook reduced

It will be noted that many features cited here were also used to characterize the Miolabinae. These features argue for a strong affiliation between the two subfamilies. We note that if further analysis suggested that they should be merged, the subfamily name Miolabinae has priority over Stenomylidae. These nine shared features outweigh the features shared between Stenomylidae and the poorly known Floridatragulinae, allied as sister subfamilies by Honey et al. (1998).

We turn next to the position of *Capricamelus* within the subfamily Miolabinae. Barghoorn (1985) developed an important concept of the Miolabinae and their diagnostic features in his unpublished doctoral dissertation. Kelly (1992) added two new genera, *Paramiolabis* Kelley, 1992, and *Cuyamacamelus* Kelley, 1992 to the subfamily. Honey et al. (1998) included these two genera, along with *Miolabis* and *Nothotylopus* Patton, 1969, in their hypothesis of phylogenetic relationships among Miolabinae.

The species included within *Paramiolabis* affect the assessment of relationships within Miolabinae. A typological contradiction arose after Kelley (1992) had designated *Paramiolabis tenuis* (Matthew, 1924) as type species, when Honey et al. (1998) cited the type as *P. singularis.* This latter usage was based on Barghoorn (1985). The prob-

Table 12 Comparative limb proportions of rock-climbing goats, goat camels, and a typical camelid.*

Element	*Rupicarpra rupicapra*	*Budorcas taxicolor*	*Oreotragus oreotragus*	*Ovis canadensis*	*Oreamnos americanus*	*Capricamelus gettyi*	*Camelops hesternus*
Humerus	344	431	369	326	409	391	333
Radius	369	399	340	371	390	393	392
Metacarpals	286	170	290	302	200	216	275
Femur	332	417	362	342	394	406	406
Tibia	413	417	408	403	426	418	349
Metatarsals	255	166	230	256	180	176	250

* Articular length of each element as a proportion of the whole limb. Data (N = 10) for five bovid species in Scott (1985). *Camelops hesternus* values are means of a large sample from Webb (1965).

lem with Barghoorn's usage is purely a legal one, in that his unpublished dissertation does not satisfy requirements for formal description under the international rules of zoological nomenclature. By the same token, Barghoorn's informal genus name "*Merychenia*" was supplanted by *Paramiolabis,* so *P. tenuis* has legal claim to be the type species, unless that species is synonymized with an earlier one. An additional species, *P. taylori,* also named by Kelley (1992), adds importantly to our understanding of the genus.

Thus there are now several well-studied samples of *Paramiolabis* from California, New Mexico, and Nebraska which range chronologically from late Hemingfordian through late Barstovian land mammal ages. Unfortunately, however, a full phylogenetic revision of the Miolabinae must still await more complete evidence of *Nothotylopus* and *Cuyamacamelus.*

The morphology of *Capricamelus* is sufficiently well known that it can be placed within the proposed cladogram of Miolabinae (Fig. 18). We recognize its sister taxon as *Paramiolabis.* Shared derived features that closely ally these two genera are as follows.

1) Elongate rostrum and with long upper and lower diastemata
2) Laterally compressed bullae
3) Upper premolars greatly reduced including P^1 vestigial or absent, P^2 absent, P^3 greatly reduced, and P^4 reduced
4) Lower premolars also reduced including P_1 and P_2 vestigial or absent and P_3 reduced or absent
5) Upper molars with flattened labial ribs and styles
6) Lower molars with flattened lingual walls and weak stylids

These two genera, *Capricamelus* and *Paramiolabis,* together comprise the progressive sister branch of *Miolabis.* as shown in Figure 18, Node 5. With respect to the six characters featured above, *Miolabis* remains more primitive than the other two genera. For example, its dental formula is complete except for loss of P_1. Also its cheek teeth are lower crowned than those of *Paramiolabis* and much lower crowned than those of *Capricamelus.* It is more difficult to place the two less adequately known miolabine genera, *Nothotylopus* and *Cuyamacamelus,* but it is fairly clear that they represent more primitive branches than *Miolabis.* We follow the arrangement for the four other genera represented by Honey et al. (1998).

The unique combination of primitive and derived features found in *C. gettyi* suggests that its lineage had a long independent history, perhaps in mountainous terrain of the Great Basin. The antiquity of this lineage can be estimated from the known chronological range of its sister genus, *Paramiolabis.* That genus, as presently known, appears in the late Hemingfordian, about 17 million years ago. For two reasons, this must be considered a minimum estimate of the divergence date of *C. gettyi.* First, the earliest known stratigraphic occurrence of the sister genus is probably younger than its actual time of origin. Second, if some of the derived features, such as loss of premolars, shared by these sister genera were acquired in parallel fashion, their time of separation may be more ancient than the range of the supposed shared derived characters in *Paramiolabis.* That might explain why the lack of fusion in the metapodials, a primitive feature seen in *Capricamelus,* is not shared with *Paramiolabis.* It is safe to say that the *Capricamelus* lineage became isolated from other miolabine stock at least 17 million years ago.

ADAPTATIONS OF *CAPRICAMELUS GETTYI*

Turning from phylogenetic concerns to adaptive scenarios, *C. gettyi* represents an extraordinary set of specializations. We show that most of its features can be interpreted as adaptations for life as a "mountain goat ecomorph." We therefore propose to call miolabines, and especially this genus, "goat camels" in the same broad sense that other groups of fossil camelids have been dubbed "gazelle camels" and "giraffe camels." We discuss first the adaptations reflected in the masticatory system of *C. gettyi* and second those of its locomotor system.

Table 13 Comparative measurements of goat and camel metapodials.

	Saiga tatarica LACM 54426	*Ovis dalli* LACM 52446	*OVIS canadensis* LACM 54187	*Oreamnos americanus* LACM 72527	*Capricamelus gettyi* (sample mean)		*Palaeolama mirifica* (Webb, 1974)
					III	IV	
MC III and IV							
Length	157.0	175.1	177.4	114.7	138.6	136.0	296
Proximal width	25.3	30.7	32.8	40.1	25.1	24.7	—
Proximal depth	17.8	20.6	22.5	26.0	27.1	26.9	—
Distal width	25.6	31.2	35.7	46.2	30.2	28.7	—
MT III and IV							
Length	176.9	190.9	190.0	132.9	115.6	117.4	263
Proximal width	21.6	26.0	27.3	36.9	20.9	20.2	—
Proximal depth	22.7	23.4	28.0	30.0	28.3	29.2	—
Distal width	24.9	30.7	32.5	47.8	26.0	25.0	—

The most striking craniodental specialization of *C. gettyi* is the battery of four, greatly enlarged upper incisors which occludes along a broad arcade with six lower incisors. Clearly this represents a powerful mechanism for incising coarse vegetation. It is broadly reminiscent of the incisor battery in *Equus* Linnaeus, 1758. Analysis of carbon isotopes recovered from *C. gettyi* tooth enamel would further illuminate the question of feeding modalities. The posterior extension of a deep premaxillary bone helps buttress these long-rooted incisors and resist torque applied to their occlusal surfaces. The very long rostrum houses very long diastemata, which provide space, as in other coarse-feeding ungulates, to manipulate masses of grass, leaves, and other coarse vegetation with the tongue in preparation for the powerful cheek battery of hypsodont molars. The loss of intervening upper teeth, including I^3, C^1, P^1, P^2, and P^3, and the reduction of P^4, and equivalent reductions in the lower dentition, was concomitant with the process of opening up the diastemata. The large subcircular fossa in the maxillary bone anterior to the orbit houses a large *M. nasolabialis* to move muscular lips that helped *C. gettyi* take in its food.

Many peculiarities of the mandible in *C. gettyi* and other miolabine camels are correlated with their distinctive feeding mode which emphasized *M. masseter* and de-emphasized *M. temporalis*. In most camelids, including extant *C. dromedarius*, the temporal area is very large, and a long coronoid process provides the area of its insertion. Such a system gives rapid action to the fighting teeth, including the last upper incisor and the canines. The importance of the temporal muscle system becomes reduced in *C. gettyi*. The deep and profound parts of the *M. masseter* are greatly expanded in Miolabinae, especially in *C. gettyi*, and this is reflected in the deep wall of maxillary and jugal bones beneath the orbit and in the expanded apron in the posteroventral portion of the mandible. The disappearance of the angular notch is a corollary of this great expansion. Not only does this powerful masseter complex give great force to the hypsodont cheek teeth, but also it translates anteriorly, as in *Equus*, to tight occlusion of the incisors.

The most remarkable features of *C. gettyi* appear in its postcranial skeleton. The overall limb proportions are far shorter than in any other camelid. As noted in the description the neck is 20% shorter than in a comparably sized *L. guanicoe*. Its tail is also short, as reflected by the probable appearance of only ten caudals in the articulated holotype skeleton, LACM 124001. The limbs are also short-coupled and very powerfully built. In the humerus the greater tuberosity is huge and towers over the posterodorsal face of that bone. The olecranon process is very thick and straight, not arched posteriorly. *Musculus biceps brachialis* is extraordinarily well developed. The distal carpal surfaces are flat, not convex, indicating that the legs were held stiff and straight.

The most extreme adaptations for a mountain goat habitus in *C. gettyi* are evident in the feet. Virtually every joint reflects a system that is tightly bound with ligaments, including joint capsules, cruciate ligaments, and interdigital ligaments. The last feature is reflected most clearly in the ungual phalanges, where facing flanges rigidly lace and brace them against impact (Fig. 12B). Likewise the fetlock joint had an extraordinarily large pair of sesamoid bones, described above, that were woven in life by short and cruciate ligaments to the plantar face of each proximal phalanx. The toes do not diverge distally as they do in all progressive camelids. The proximal phalanges did not reach the ground and did not flex upward around the anterior face of each corresponding metapodial as they do in later digitigrade camelids. The feet of *C. gettyi* also lack the elaborate set of cushioned pads that support the digitigrade feet, as described for *C. dromedarius* by Arnautovic and Abdalla (1969). No camelids have distal sesamoids at the coffin joint, and although they probably would have served a useful function in these goat camels as the "navicular sesamoids" do in horses and ruminants, their absence is confirmed in the numerous well-preserved feet of *C. gettyi*. In every way the limbs of *C. gettyi* bespeak adaptations for low-gear locomotion closely convergent with those of mountain goats.

A broader indication of adaptive convergence between *C. gettyi* and mountain goats can be read from its limb proportions. Table 12 presents a comparative array of relevant limb proportions selected from the comprehensive survey of bovid limb proportions and locomotor adaptations of Scott (1985). She showed that similar low-gear systems, categorized as "true rock climbers," evolved independently in several parts of the world. These include the chamois (*Rupicapra rupicapra* (Linnaeus, 1758)) from mountains in Europe and Asia Minor, the takin (*Budorcas taxicolor* Hodgson, 1850) from southeast Asia, the klipspringer (*Oreotragus oreotragus* (Zimmerman, 1783)) from Africa, and the North American mountain goat (*Oreamnos americanus* (Blainville, 1816)). The bighorn sheep of North America (*Ovis canadensis* (Shaw, 1804)) is also included in Table 12 for comparison but is considered merely "an inhabitant of rocky areas" by Scott (1985), but not a true rock climber. In its forelimb proportions *C. gettyi* falls nearest *O. americanus* and between it and *O. oreotragus*. Only *B. taxicolor* has a relatively shorter metacarpus. Likewise in the hind limb, *C. gettyi* most nearly resembles *Oreamnos*, although *C. gettyi* has even stockier proportions than that genus. As in the forelimb, only *B. taxicolor* has proportionally shorter metapodials than *C. gettyi*. In each of these rock-climbing ruminants, the tibia is the longest bone, and the metatarsals range from just over to just under half of its length; *C. gettyi* adheres to this pattern.

Table 13 presents measurements of metapodials in various extant goatlike ruminants compared with those of *C. gettyi* and *Palaeolama mirifica* (Simpson, 1929), the "short-legged llama." Note that the closest comparisons are again between *C. gettyi* and *O. americanus*. A curious difference, however, is that in *C. gettyi* the metacarpal is considerably longer and wider than the metatarsal, whereas the reverse is true in *O. americanus*. This heavier construction of the forelimb occurs throughout the Camelidae and presumably is correlated with their relatively long necks and powerful forequarters. Compared with other Camelidae, *C. gettyi* has by far the shortest distal limb elements known. For example, as seen in Table 13, *P. mirifica*, despite its title as the short-legged llama and a body weight roughly equal to that of *C. gettyi*, has metapodials more than twice the length of those of *C. gettyi*.

CONCLUSIONS

Capricamelus gettyi is a very distinctive new genus and species that sheds light on the broader relationships and adaptive trends within the Camelidae. In particular it represents a highly specialized member of the subfamily Miolabinae and suggests a sister group relationship between that subfamily and the Stenomylinae. Its cranium has a long rostrum with a powerful battery of upper and lower incisors, followed by a very long diastema, associated with the absence of five upper and four lower intermediate teeth and a set of very hypsodont, transversely compressed molars. Several peculiarities of the mandible, including expansive posteroventral apron, absence of angular hook, and abbreviated coronoid process, correlate with expanded masseter and reduced temporal musculature compared with all other groups of camelids.

The most distinctive features of *C. gettyi*, as the name suggests, appear in its short-coupled postcranial skeleton (Fig. 19). Its neck is 25% shorter than in comparably sized *L. guanicoe*, and its extremely short distal limb elements have the same proportions as in *Oreamnos*, the mountain goat. Although *Capricamelus* is the most specialized goat camel, it can be considered the end member of trends seen in other miolabine camelids, such as enlarged I^1 and I^2, unfused metapodials, reduced cervical vertebrae, and deep, narrowly compressed bullae. The presence of unfused metapodials in animals whose feet are otherwise so fully consolidated is puzzling and must indicate some deep genetic inability to produce fused cannon bones so prevalent in most other camelid taxa, even in many of the Miocene Stenomylinae. It suggests that this branch of goat camels arose early in the Miocene from some stock about as ancient as *Stenomylus* itself.

The locus of the one fortuitous sample of *C. gettyi* provides a clue as to its presumed long absence from the known record. Its occurrence in part of the Great Basin in a semiarid region surrounded by high mountains tends to corroborate its adaptive

Figure 19 Reconstruction of *Capricamelus gettyi* showing goatlike adaptations of short, goatlike limbs and foreshortened neck

morphology that converges postcranially with mountain goats. We conclude that these goat camels lived for some 20 million years in mountainous parts of western North America.

ACKNOWLEDGMENTS

First and foremost, we extend our gratitude to Mr. Andrew R. Getty for his support of and interest in this study. Many staff and volunteers of the Natural History Museum of Los Angeles County spent long days and nights quarrying the specimens described in this study, but we wish to particularly acknowledge the efforts of Harley Garbani, Joe Cocke, and Michael T. Greenwald. Mike Woodburne and students from the University of California, Riverside, also provided field assistance. Paleontology Section preparators Mary J. Odano, D.B. Joe Cocke, and Michael K. Hammer prepared most of the material, and Joe Cocke returned from retirement to complete preparation for this study. Specimen illustrations and the artistic reconstruction were prepared by Christina Wioch. Graphic illustration assistance was provided by Steven Melendrez. Computer enhancing of artwork was provided by Richard Meier, Angelica Oliva, William Mertz, and Audrey Adams. Partial support was provided by NSF grant DEB 72–02014. Additional field support was provided by the Natural History Museum of Los Angeles County Foundation. The authors benefited from discussions with many colleagues over the years, but we wish to particularly acknowledge Richard H. Tedford, James Honey, Christine Janis, and David E. Fortsch. Bill Akersten and Susanne J. Miller brought to our attention the additional specimen from Smith Creek Cave, and Amy Dansie at the Nevada State Museum kindly loaned us this specimen for

comparative study. Richard H. Tedford brought our attention to the additional specimens in the American Museum of Natural History, and our studies greatly benefited from comparisons with specimens within the Frick collections there. John Harris, Gordon Hendler, James Honey, Inez Horrowitz, Donald Prothero, and Xiaoming Wang provided valuable review comments.

LITERATURE CITED

Arnautovic, M.M., and S.M. Abdalla. 1969. The elastic structure of the foot of the camel. *Acta Anatomica* 72(3):411–428.

Barghoorn, S.F. 1985. *Magnetic polarity stratigraphy of the Tesuque Formation, Santa Fe Group in the Espanola Valley, New Mexico, with a taxonomic review of the fossil camels.* Ph.D. Thesis. New York: Columbia University.

Chesterman, C.W. 1973. *Geology of the northeast quarter of Shoshone Quadrangle, Inyo County, California.* California Division of Mines and Geology, Map Sheet 18. San Francisco, CA.

Cope, E.D. 1876. On a new genus of Camelidae. *Proceedings of the Academy of Natural Sciences of Philadelphia* 28:144–147.

Dohrenwend, J.W. 1985. Patterns and processes of middle and late Quaternary dissection in the Lake Tecopa basin. In *1985 Annual field trip guidebook: California: Friends of the Pleistocene, Pacific Cell,* 113–144. Santa Ana, CA.

Dohrenwend, J.W., W.B. Bull, L.D. McFadden, G.I. Smith, R.S. Smith, and S.G. Wells. 1991. Quaternary geology of the Basin and Range Province in California. In *Quaternary nonglacial geology, conterminous United States, decade of North American geology, Bulletin Geological Society of America,* ed. R.B. Morrison, vol. K-2, 321–352. Boulder, CO.

Frick, C. 1937. Horned ruminants of North America. *Bulletin of the American Museum of Natural History* 69:1–669.

Frick, C., and B.E. Taylor. 1968. A generic review of the stenomyline camels. *American Museum Novitates* 2353:1–51.

Gazin, C.L. 1934. Fossil hares from the late Pliocene of southern Idaho. Proceedings, U.S. National Museum 83:111–121.

Gervais, H., and F. Ameghino. 1880. *Les mammiferes fossiles de l'Amerique du Sus.* Paris: Library F. Sary.

Gidley, J.W. 1922. Preliminary report on fossil vertebrates of the San Pedro Valley, Arizona, with descriptions of new species of rodents and lagomorphs. *U.S. Geological Survey Professional Paper* 131E:119–131.

Hay, O.P. 1902. Bibliography and catalog of the fossil Vertebrata of North America. *Bulletin of the United States Geological Survey* 179:5–868.

Hillhouse, J.W. 1987. *Late Tertiary and Quaternary geology of the Tecopa Basin, southeastern California.* United States Geological Survey Miscellaneous Investigation Map I-1728. Cambridge, UK.

Honey, J.G., J.A. Harrison, D.R. Prothero, and M.S. Stevens. 1998. Camelidae. In *Evolution of Tertiary mammals of North America,* vol. 1; *Terrestrial carnivores, ungulates and ungulate-like mammals,* ed. C. Janis, K. Scott, and L. Jacobs, 439–462. Cambridge University Press, Cambridge, UK.

Illiger, C. 1811. *Prodromus systematicus mammalium et avium additis terminis zoographicus utriusque classis.* Berlin: C Salfeld.

James, B. 1985. *Late Pliocene (Blancan) nonmarine and volcanic stratigraphy and microvertebrates of Lake Tecopa, California.* Unpublished Masters Thesis. Department of Earth Sciences, University of California, Riverside.

Kelly, T.S. 1992. New middle Miocene camels from the Caliente Formation, Cuyama Valley badlands, California. *PaleoBios* 13:1–22.

Larson, E.E. 2000. Sedimentology and stratigraphy of the Plio-Pleistocene Lake Tecopa beds, southeastern California. In *Empty basins, vanished lakes,* ed. R.E. Reynolds and J. Reynolds. San Bernardino County Museum Association, vol. 47, no. 2, 56–62.

Larson, E.E., and P.E. Patterson. 1993. The Matuyama-Brunhes reversal at Tecopa basin, southeastern California, revisited again. *Earth and Planetary Science Letters* 120:311–325.

Larson, E.E., P.E. Patterson, and F. Luiszer. 1991. Paleoclimatic record from 2.4 to 0.5 Ma, Tecopa basin, southeastern California. *Geological Society of America, Abstracts with Programs* 23:120.

Leidy, J. 1847. On a new genus and species of fossil Ruminantia. *Proceedings of the Academy of Natural Sciences of Philadelphia* 3:322–326.

———. 1854. Description of a fossil apparently indicating an extinct species of the camel tribe. *Proceedings of the Academy of Natural Sciences of Philadelphia* 7: 172–173.

———. 1869. The extinct mammalian fauna of Dakota and Nebraska including an account of some allied forms from other localities, together with a synopsis of the mammalian remains of North America. *Journal of the Academy of Natural Sciences of Philadelphia* 7:1–472.

MacFadden, B.J. 1998. Equidae. In *Evolution of Tertiary mammals of North America,* vol. 1; *Terrestrial carnivores, ungulates and ungulate-like mammals,* ed. C. Janis, K. Scott, and L. Jacobs, 537–559. Cambridge University Press, Cambridge, UK.

Matthew, W.D. 1924. Third contribution to the Snake Creek fauna. *Bulletin of the American Museum of Natural History* 50:59–210.

Miller, S.J. 1979. The archeological fauna of four sites in Smith Creek Canyon. In *The archeology of Smith Creek Canyon, Nevada,* ed. D.R. Tuohy and D.L. Rendall, chap. 5. Nevada State Museum, Anthropological Papers, vol. 17, 272–329.

Morrison, R.B. 1991. Quaternary geology of the southern Great Basin, with emphasis on Lakes Lahontan, Bonneville and Tecopa. In *Quaternary nonglacial geology, conterminous United States, decade of North American geology,* ed. R.B. Morrison. Bulletin Geological Society of America, vol. K-2, chap. 10, 283–320.

———. 1999. Lake Tecopa: Quaternary geology of the Tecopa Valley, California, a multimillion-year record and its relevance to the proposed nuclear-waste repository at Yucca Mountain, Nevada. In *Cenozoic basins of the Death Valley region,* ed. L.A. Wright and B.W. Troxel. Geological Society of America, Special Paper 333, 301–344.

North American Stratigraphic Code. 1983. The North American Commission on Stratigraphic Nomenclature. *The American Association of Petroleum Geologists Bulletin* 67(5):841–875.

Owen, R. 1848. Description of teeth and portions of jaws of two extinct Anthracotherioid quadrapeds (*Hyopotamys vectianus* and *H. bovinus*) discovered by the Marchioness of Hastings in the Eocene deposits

on the N.W. coast of the Isle of Wright: With an attempt to develop Cuvier's idea of the classification of pachyderms by the number of their toes. *Quaternary Journal of the Geological society of London* 4: 103–141.

Patton, T.H. 1969. Miocene and Pliocene artiodactyls, Texas Gulf Plain. *Bulletin of the Florida State Museum* 14:115–227.

Peterson, O.A. 1904. Osteology of *Oxydactylus*. *Annals of the Carnegie Museum* 2:434–476.

———. 1906. The Miocene beds of eastern Nebraska and western Wyoming and their faunae. *Annals of the Carnegie Museum* 4:21–72.

———. 1908. Description of the type specimen of *Stenomylus gracilis* Peterson. *Annals of the Carnegie Museum* 4:286–300.

Reynolds, R.E. 1991. The Shoshone Zoo: A Rancholabrean assemblage from Tecopa. In *Crossing the borders: Quaternary studies in eastern California and southwestern Nevada,* ed. R.E. Reynolds. Special Publication, San Bernardino County Museum Association, 159–162.

Sarna-Wojicicki, A.M., H.R. Bowerman, C.E. Meyer, P.C. Russell, M.J. Woodward, G. McCoy, J.J. Rowe, P.A. Baedecker, F. Asaro, and H. Michael. 1987. Chemical analyses, correlations, and ages of Upper Pliocene and Pleistocene ash layers of east-central and southern California. *United States Geological Survey Professional Paper* 1293:1–40.

Scott, K.M. 1985. Allometric trends and locomotor adaptations in the Bovidae. *Bulletin of the American Museum of Natural History* 179:197–288.

Shepard, R.A., and A.J. Gude III. 1968. Distribution and genesis of authigenic silicate minerals in tuffs of Pleistocene Lake Tecopa, Inyo County, California. *United States Geological Survey Professional Paper* 597:1–37.

Simpson, G.G. 1929. Pleistocene mammalian fauna of the Seminole Field, Pinellas County, Florida. *Bulletin of the American Museum of Natural History* 56(8): 561–599.

Smuts, M.S., and R.J. Bezuidenhout. 1987. *Anatomy of the dromedary.* Oxford University Press, London, UK. 230 pp.

Stock, C. 1936. A new mountain goat from the Quaternary of Smith Creek Cave, Nevada. *Bulletin, Southern California Academy of Sciences* 35(3):149–152.

Valet, J.P., L. Tauxe, and D.R. Clark. 1988. The Matuyama-Brunhes transition recorded from Lake Tecopa sediments (California). *Earth and Planetary Science Letters* 87:463–472.

Van Couvering, J.A. 1997. Preface: The new Pleistocene. In *The Pleistocene boundary and the beginning of the Quaternary,* ed. J.A. Van Couvering, xi–xvii. Cambridge University Press, Cambridge, UK.

Webb, S.D. 1965. The osteology of *Camelops*. *Bulletin of the Los Angeles County Museum. Science* 1:1–54.

Webb, S.D., and B.E. Taylor. 1980. The phylogeny of hornless ruminants and a description of the cranium of *Archaeomeryx*. *Bulletin of the American Museum of Natural History* 167:121–157.

Woodburne, M.O., and D.P. Whistler. 1991. The Tecopa lake beds. In *Crossing the borders: Quaternary studies in eastern California and southwestern Nevada,* ed. R.E. Reynolds. Special Publication, San Bernardino County Museum Association, 155–157.

Received 3 April 2002; accepted 6 July 2004.

Appendix Hypodigm of *Capricamelus gettyi* from locality LACM 7111.

LACM	27477	L	Pes
LACM	27478	L	Humerus dist + ulna prox + radius + frags
LACM	27479	R	Tibia dist + fibula + pes
LACM	27480		Skull and W L + R I1–2 + L + R dentary ant w il-c
LACM	27481	L	Tibia dist + fibula + tarsals + metatarsal III–IV + 3 sesamoids
LACM	27482	R	Skull mid w M1–M3 + R Dentary post w m2–m3
LACM	122333	L	Radio-ulna dist + manus
LACM	123964	L	Radio-ulna + manus
LACM	123965	R	Humerus dist + radio-ulna + manus
LACM	123966	R	Humerus dist + radio-ulna + manus
LACM	123967	L	Radio-ulna frags + manus
LACM	123968	R	Tibia + fibula + pes
LACM	123969	R	Tibia + pes incompl
LACM	123970	L	Metatarsal III–IV + digit III–IV + Sesamoids 4
LACM	123971		Metatarsal dist frags + digit III–IV
LACM	123972	L	Radio-ulna dist + manus
LACM	123973	R	Radius dist + manus
LACM	123974	R	Manus
LACM	123975	L	Manus
LACM	123976		Tarsus phalanx I + II + III + frags
LACM	123977		Metatarsal III–IV + digit III–IV prox + sesamoids
LACM	123978		Skull + skeleton
LACM	123999	L+R	Radio-ulna + manus
LACM	124000	L+R	Radio-ulna dist + manus + R humerus dist
LACM	124001		Sacrum + vertebrae caudal + innominate + hind limb
LACM	124002		Skull + skeleton
LACM	124003	L	Humerus + radio-ulna + manus
LACM	124004		Phalanx prox + med + dist
LACM	145102	R	Dentary w di1–di3
LACM	145103		Lumbar vertebrae
LACM	145104	L	Astragalus
LACM	145105	L	Astragalus
LACM	145106	L	Astragalus
LACM	145107	L	Astragalus
LACM	145108	R	Astragalus
LACM	145109	R	Astragalus
LACM	145110	R	Astragalus frag
LACM	145111	R	Astragalus frag
LACM	145112	R	Astragalus frag
LACM	145113	R	Astragalus frag
LACM	145114	R	Astragalus frag
LACM	145115	R	Astragalus frag
LACM	145116	R	Astragalus frag
LACM	145117	L	Calcaneum
LACM	145118	L	Calcaneum frag
LACM	145119	L	Calcaneum frag
LACM	145120	R	Calcaneum frag
LACM	145121	R	Calcaneum frag
LACM	145122	L	Patella
LACM	145123	L	Patella
LACM	145124	L	Patella
LACM	145125	L	Patella
LACM	145126	L	Patella frag
LACM	145127	R	Patella
LACM	145128	R	Patella
LACM	145129	R	Patella frag
LACM	145130	R	Patella frag
LACM	145131		Metatarsal III

Appendix Continued.

LACM	145132	Phalanx proximal
LACM	145133	Phalanx proximal
LACM	145134	Phalanx proximal
LACM	145135	Phalanx Proximal
LACM	145136	Phalanx proximal
LACM	145137	Phalanx proximal
LACM	145138	Phalanx proximal frag
LACM	145139	Phalanx proximal frag
LACM	145140	Phalanx proximal frag
LACM	145141	Phalanx proximal frag
LACM	145142	Phalanx proximal frag
LACM	145143	Phalanx proximal frag
LACM	145144	Phalanx proximal frag
LACM	145145	Phalanx proximal frag
LACM	145146	Phalanx proximal frag
LACM	145147	Phalanx proximal frag
LACM	145148	Phalanx proximal frag
LACM	145149	Phalanx proximal frag
LACM	145150	Phalanx proximal frag
LACM	145151	Phalanx proximal frag
LACM	145152	Phalanx proximal frag
LACM	145153	Phalanx proximal frag
LACM	145154	Phalanx proximal frag
LACM	145155	Phalanx proximal frag
LACM	145156	Phalanx proximal frag
LACM	145157	Phalanx proximal frag
LACM	145158	Phalanx proximal frag
LACM	145159	Phalanx proximal frag
LACM	145160	Phalanx proximal frag
LACM	145161	Phalanx proximal frag
LACM	145162	Phalanx proximal frag
LACM	145163	Phalanx proximal frag
LACM	145164	Phalanx proximal frag
LACM	145165	Phalanx proximal epiphysis proximal
LACM	145166	Phalanx medial
LACM	145167	Phalanx medial
LACM	145168	Phalanx medial
LACM	145169	Phalanx medial
LACM	145170	Phalanx medial
LACM	145171	Phalanx medial
LACM	145172	Phalanx medial
LACM	145173	Phalanx medial
LACM	145174	Phalanx medial
LACM	145175	Phalanx medial
LACM	145176	Phalanx medial
LACM	145177	Phalanx medial
LACM	145178	Phalanx medial
LACM	145179	Phalanx medial
LACM	145180	Phalanx medial
LACM	145181	Phalanx medial
LACM	145182	Phalanx medial
LACM	145183	phalanx medial
LACM	145184	Phalanx medial
LACM	145185	Phalanx medial
LACM	145186	Phalanx medial frag
LACM	145187	Phalanx medial frag
LACM	145188	Phalanx medial frag
LACM	145189	Phalanx medial frag

Appendix Continued.

LACM	145190	Phalanx medial frag
LACM	145191	Phalanx medial frag
LACM	145192	Phalanx medial frag
LACM	145193	Phalanx medial frag
LACM	145194	Phalanx medial frag
LACM	145195	Phalanx medial frag
LACM	145196	Phalanx medial frag
LACM	145197	Phalanx medial frag
LACM	145198	Phalanx medial frag
LACM	145199	Phalanx medial frag
LACM	145200	Phalanx medial frag
LACM	145201	Phalanx medial frag
LACM	145202	Phalanx medial frag
LACM	145203	Phalanx medial frag
LACM	145204	Phalanx medial frag
LACM	145205	Phalanx medial frag
LACM	145206	Phalanx medial frag
LACM	145207	Phalanx medial frag
LACM	145208	Phalanx medial frag
LACM	145209	Phalanx medial frag
LACM	145210	Phalanx medial frag
LACM	145211	Phalanx medial frag
LACM	145212	Phalanx medial frag
LACM	145213	Phalanx medial frag
LACM	145214	Phalanx medial frag
LACM	145215	Phalanx medial frag
LACM	145216	Phalanx medial frag
LACM	145217	Phalanx medial frag
LACM	145218	Phalanx ungual
LACM	145219	Phalanx ungual
LACM	145220	Phalanx ungual
LACM	145221	Phalanx ungual
LACM	145222	Phalanx ungual
LACM	145223	Phalanx ungual
LACM	145224	Phalanx ungual
LACM	145225	Phalanx ungual
LACM	145226	Phalanx ungual
LACM	145227	Phalanx ungual
LACM	145228	Phalanx ungual
LACM	145229	Phalanx ungual frag
LACM	145230	Phalanx ungual frag
LACM	145231	Phalanx ungual frag
LACM	145232	Phalanx ungual frag
LACM	145233	Phalanx ungual frag
LACM	145234	Phalanx ungual frag
LACM	145235	Phalanx ungual frag
LACM	145236	Phalanx ungual frag
LACM	145237	Phalanx ungual frag
LACM	145238	Phalanx ungual frag
LACM	145239	Phalanx ungual frag
LACM	145240	Phalanx ungual frag
LACM	145241	Phalanx ungual frag
LACM	145242	Phalanx ungual frag
LACM	145243	Phalanx ungual frag
LACM	145244	Phalanx ungual frag
LACM	145245	Phalanx ungual frag
LACM	145246	Phalanx ungual frag
LACM	145247	Ectocuneiform

Appendix Continued.

LACM	145248	Ectocuneiform
LACM	145249	Navicular
LACM	145250	Navicular
LACM	145251	Navicular
LACM	145252	Navicular
LACM	145253	Navicular
LACM	145254	Cuboid
LACM	145255	Cuboid
LACM	145256	Cuboid
LACM	145257	Cuboid
LACM	145258	Cuboid
LACM	145259	Cuboid
LACM	145260	Cuboid
LACM	145261	Cuboid
LACM	145262	Metacarpal dist
LACM	145263	Metacarpal dist
LACM	145264	Metacarpal dist
LACM	145265	Metacarpal dist
LACM	145266	Metacarpal dist
LACM	145267	Metacarpal dist
LACM	145268	Metacarpal dist
LACM	145269	Metacarpal dist
LACM	145270	Metacarpal dist
LACM	145271	Metacarpal dist
LACM	145272	Metatarsal dist
LACM	145273	Metatarsal dist
LACM	145274	Metatarsal dist
LACM	145275	Metatarsal dist
LACM	145276	Metatarsal dist
LACM	145277	Metatarsal dist
LACM	145278	Metatarsal dist
LACM	145279	Metatarsal dist
LACM	145280	Metatarsal dist
LACM	145281	Metatarsal dist
LACM	145282	Metatarsal dist
LACM	145283	Metatarsal dist
LACM	145284	Metatarsal dist
LACM	145285	Metatarsal dist
LACM	145286	Metatarsal dist
LACM	145287	Fibula
LACM	145288	Fibula
LACM	145289	Fibula
LACM	145290	Fibula
LACM	145291	Tibia prox
LACM	145292	Tibia prox
LACM	145293	Tibia prox
LACM	145294	Tibia prox
LACM	145295	Tibia prox
LACM	145296	Tibia prox
LACM	145297	Tibia dist
LACM	145298	Tibia dist
LACM	145299	Tibia dist
LACM	145300	Tibia dist
LACM	145301	Tibia dist
LACM	145302	Tibia dist
LACM	145303	Metapodial proximal frag
LACM	145304	Metapodial proximal frag
LACM	145305	Metapodial proximal frag

Appendix Continued.

LACM	145306	Metapodial proximal frag
LACM	145307	Metapodial proximal frag
LACM	145308	Metapodial proximal frag
LACM	145309	Metapodial proximal frag
LACM	145310	Metapodial proximal frag
LACM	145311	Metapodial proximal frag
LACM	145312	Metapodial proximal frag
LACM	145313	Metapodial proximal frag
LACM	145314	Metapodial proximal frag
LACM	145315	Metapodial proximal frag
LACM	145316	Calcaneum frag
LACM	145317	Calcaneum frag
LACM	145318	Calcaneum frag
LACM	145319	Calcaneum frag
LACM	145320	Calcaneum frag
LACM	145321	Calcaneum frag
LACM	145322	Calcaneum frag
LACM	145325	Unciform
LACM	145326	Unciform
LACM	145327	Unciform
LACM	145328	Unciform
LACM	145329	Unciform
LACM	145330	Unciform
LACM	145331	Scaphoid
LACM	145332	Scaphoid
LACM	145333	Scaphoid
LACM	145334	Scaphoid
LACM	145335	Magnum
LACM	145336	Cuneiform
LACM	145337	Cuneiform
LACM	145338	Cuneiform
LACM	145339	Cuneiform
LACM	145340	Cuneiform frag
LACM	145341	Cuneiform frag
LACM	145342	Lunar
LACM	145343	Lunar
LACM	145344	Lunar
LACM	145345	Lunar
LACM	145346	Lunar
LACM	145347	Lunar
LACM	145348	Innominate frag
LACM	145349	Innominate frag
LACM	145350	Innominate frag
LACM	145351	Femur frag
LACM	145352	Femur frag
LACM	145353	Femur frag
LACM	145354	Femur frag
LACM	145355	Femur frag
LACM	145356	Femur frag
LACM	145357	Femur frag
LACM	145358	Femur frag
LACM	145359	Femur frag
LACM	145360	Femur frag
LACM	145361	Femur frag
LACM	145362	Pisiform
LACM	145363	Pisiform
LACM	145364	Pisiform
LACM	145365	Pisiform

Appendix Continued.

LACM	145366	Pisiform
LACM	145367	Pisiform
LACM	145368	Trapezoid
LACM	145369	Trapezoid
LACM	145370	Trapezoid
LACM	145371	Trapezoid
LACM	145372	Trapezoid
LACM	145373	Trapezoid
LACM	145374	Trapezoid
LACM	145375	Trapezoid
LACM	145376	Scapula
LACM	145417	Metapodial proximal frag
LACM	149589	Skull reconstructed model

Natural History Museum
of Los Angeles County
900 Exposition Boulevard
Los Angeles, California 90007